Journal of Engineering and Technology
of the Open University of Sri Lanka

Volume 05 No. 02 September 2017 ISSN 2279-2627

All correspondence should be addressed to:

Editor in Chief- Journal of Engineering and Technology
Faculty of Engineering Technology
The Open University of Sri Lanka
Nawala, Nugegoda
Sri Lanka
Email: meper@ou.ac.lk, Telephone: +94112881061

The Journal of Engineering and Technology of the Open University of Sri Lanka is a peer-reviewed journal published bi-annually by the Faculty of Engineering Technology of the Open University of Sri Lanka. The Journal accepts original articles based on theoretical and applied research in the area of Engineering and Technology in all specializations.

Published in June 2018.

CONTENTS

Volume 05 No. 02 September 2017 ISSN 2279-2627

Page

Emotion Recognition and Expression Based on Human Motion in Service Robot Eye 1-15
(E. J. G. S. Appuhamy, B.G.D.A. Madushanka)

Bluetooth Low Energy Local Positioning for Museum Navigation 16-29
(N.D.C.D. Kannangara, W.D.S.S. Bandara)

Feasibility Study of Concentrating Solar Power Plant for Sri Lanka 30-43
(E.M. Asanka Jayasundara, K.A.C. Udayakumar)

A Novel Methodology for Usability Assessment of Engineering Design 44-57
(A.G.P. Lankathilaka, P.D.S.H. Gunawardane, Nimali T. Medagedara)

Emotion Recognition and Expression Based on Human Motion in Service Robot Eye

E. J. G. S. Appuhamy, B.G.D.A. Madushanka*

Department of Mechanical Engineering, The Open University of Sri Lanka, Nawala, Nugegoda, Sri Lanka.

*Corresponding Author: email: bgmad@ou.ac.lk , Tele: +94112881265

Abstract *– Service robots are developed with the assistance of rapidly growing aging and disabled population due to busy lifestyles of the human. Emotion recognition applications of service robots are still in developing stage. Service robot eye gets vision input to the intelligent system and finally give an output signal to the interaction part of the service robot. Therefore, robot eye design is an important factor to develop an accurate interacting service robot to care elders and disables. This paper introduces a method to develop an interactive service robot eye which has the capability to emotional recognition and expression based on the human motion by using haar cascade classification. Happy, sad and relax are the emotion types that elders and disables perform frequently. Therefore, intelligent system was developed to sense those emotions by training different classifiers for each emotion type. Parameters for haar classifier training involves the behavior of full body of the person by using the shapes of faces, hands, and legs. Developed robot eye was implemented and tested with different persons and finally, the results of the experiment are presented with the accuracy of the intelligent system to each tested person. According to the results, the emotions are detected more than 65% overall accuracy for each person.*

Keywords*: Domestic environment, Emotion recognition, Haar classification, Robot eyes, Service robotics*

1 INTRODUCTION

A service robot is a robot which operates semi or fully autonomously to perform services useful to the well-being of humans (Ceccarelli, 2012). A significant growth of research and development on the field of service robots has been experienced in the recent past. The annual growth rate of the variety of application opportunities for service robotics and the number of potential users increased to 11.5 percent (Lamberti et al., 2016). Latest service robotics offers welcome assistance to people while performing household chores to helping the sick, elderly or disabled. The elderly and disabled population has grown rapidly over the past several decades (Suryadevara and Mukhopadhyay, 2015). Sri Lankan society enriched with the culture of caring for the elderly by family members. However, with the change of traditional living patterns as migration, a shift to a nuclear family structure and increasing dual-earning households necessitates and migration of young talented caregivers as a labour force, increase the disabled and elderly percentage of isolated. Therefore, most of them need physical and cognitive assistance from caregivers. Shortage of caregivers will become a serious problem in near future. Therefore, service robots are developed as a solution to the crisis of caregivers with the rapid rise of disabled and elderly population in busy lifestyles (Sirithunge et al., 2017).

Emotion is a sequence of alterations. Some of them are anger, sadness, happiness, fear, surprise, disgust and tease. (Tosa and Nakatsu, 1996). Emotion can be defined as a consecutive and not in a static state. In our daily life interactions, the communication assumed by 55% of body language (Dammak, Ammar, and Alimi, 2012). Emotions and expression play an important role in how we think and behave in the day to day activities. The emotions we feel each day can compel us to act and influence the decisions we make about our lives, both large and small. Mainly emotions are expressed through verbal expression and nonverbal expression. As an example of verbal communication, by seeing that someone is crying, for instance, we might assume that he or she is in the sad mood. Nonverbal communication has been defined as communication without words. It includes apparent behaviours such as facial expressions, gestures, gait, physiological signals, linguistic information and acoustic features. Although verbal output can be turned off, nonverbal output cannot. Even silence speaks. To care persons, the robot must have an idea of emotional states of them. Many of researchers try to invent different kinds of service robots to replace caregivers, especially with voice recognition. But it couldn't use for deaf and dumb persons. Deaf and dumb persons can't give a voice response to the service robots. When they try to communicate with others, they are unable. However, they can communicate easily with others by using different body postures, facial expressions etc.

Computer-based emotion recognition is a growing field which develops new needs in terms of software modelling and integration of existing multimedia models. There must be a strong emotion classification system to distinguish one emotional state from another to recognize emotions (Wickramaratne, Buddhika, and Jayasekara, 2017). But emotion recognition technology is still in the developing stage (Laranjeira et al., 2016). Recently human emotion recognition systems have become one of the most prominent technologies in the field of human-robot interfaces. Such systems are used for maintaining an effector communication process between human and anthropomorphic robot since the emotional reaction is one the most natural communication channels used by people.

The human eye has been called the most complex organ and the most important sense in the body (Han, 2017). The eyes bring colourful sights to the people to see the beauty of the life. Rapid and accurate eye movements are crucial for the coordinated direction of gaze. Still human couldn't develop a perfect identical eye to human eye. Stereo vision, high frames per second, flexibility, instant reactions increase the complexity of human eyes. Robot eye must be binocular, active, wide field of view and it must have high-resolution capabilities to achieve the complexities of the human visual system. Human eyes have more than two degrees of freedom, but the pan and tilt movements are sufficient to scan the visual space (Maes et al., 1996).

Therefore, this paper proposes a method for developing an interactive service robot eye which has the capability for emotional recognition and expression based on human motion especially focusing the deaf and dumb persons. The overall function of the proposed robot eye is explained in section 2. The proposed methodology to emotion recognition robot eye based on human motion is explained in section 3. Experimental results are presented and discussed in section 4 according to emotion recognition process. Finally, the conclusion is presented in section 5.

2 SYSTEM OVERVIEW

Controlling mechanism of the robot eye is shown in figure 1. Rotation of the robot eye is an involuntary response of the human vision system. It has more complex eye movements. Binocular vision with two degrees of freedom eye movements helps to get the robot eye common pan and tilt movements with more human-like manner. It facilitates tasks such as reaching and grasping performed with close targets. The main effect of binocular viewing is to reduce the time taken for the task (Hayhoe et al, 2009). Field of view of the web camera that used to robot eye is 60 degrees (Logitech, 2017). Therefore, by using binocular vision, the displaying range of service robot eye can be increased. So, two web cameras are used to reach vision requirement for the robot eye to give vision input for the intelligent system for the process of emotion recognition. Servo motors are used as actuators for the system. Mechanical stops were included on each robot eye to permit a 120-degree pan rotation and a 60-degree tilt rotation to approximate the range of motion of human eyes (Komogortsev *et al.* 2012). Therefore, each robot eye rotates 60 degrees to the left and right in pan axis and 30 degrees for up and down in tilt axis during implementation. An Arduino microcontroller is used to control the servo motors. Serial communication between personal computer and microcontroller help to accurately focus robot eye on the human emotional states. A printer cable is used to build communication between the PC and the microcontroller.

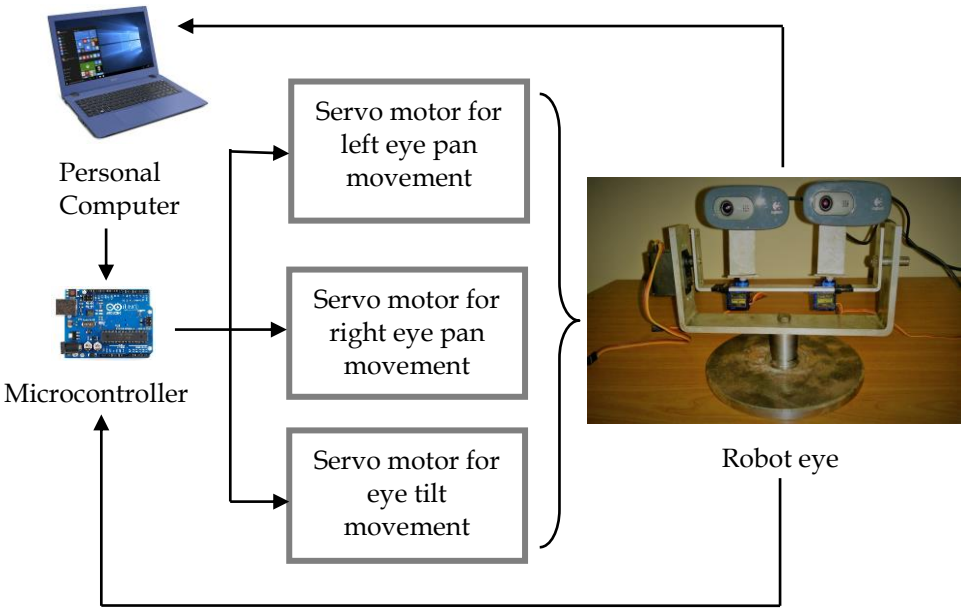

Figure 1: Controlling mechanism of the robot eye

3 EMOTION RECOGNITION ROBOT EYE BASED ON HUMAN MOTION

An intelligent system is developed to perform main processing task in the research project. Vision feedback from the two webcams is taken as the input to the intelligent system. Algorithms were developed to search, detect, focus person's emotional states by using openCV, visual studio C++ and haar cascade classifier. In the beginning, the robot eye is continuing searching an emotional state. If it is detected emotional state like haar cascade classifier that trained, then the robot eye focus to it. Emotions are limited in the trained intelligent system. They are focused to detect three emotions types. They are happiness, sadness and relax. Because they are the widely accepted and recognized emotions for elders and disables. The emotions are classified according to those body

postures of the human by using the shape of faces, hands, and legs, relevant to each emotion type. Figure 2, figure 3, and figure 4 shows all the types of body postures related to emotions which detect by the intelligent system under relaxing mood sad mood, and happy mood. Shapes of hands, faces and legs are used to classify emotions according to the body postures.

Figure 2: All the types of body postures that trained for relaxing mood

Figure 3: All the types of body postures that trained for happy mood

Figure 4: All the types of body postures that trained for sad

3.1 Implement the Robot Eye Movement Focus to an Emotion of a Person

Implementation of the intelligent system can be shown in Fig. 5. The methodical approach is done by using four stages. First, design and development of robot eye with pan-tilt movement to reach more human-like. Second, identify the emotional status used in daily activities by elderly and disable in the domestic environment by using their body postures. Next, develop an intelligent system for understanding emotional status. Data classification, serial communication between intelligent system and microcontroller, tracking and focusing on human emotions are the common features of the intelligent system. All the recognized emotional states are classified in this context memory as sad mood, relax mood and happy mood. Finally, test the developed intelligent system with the service robot eye in the domestic environment by using three persons to check the accuracy of the system.

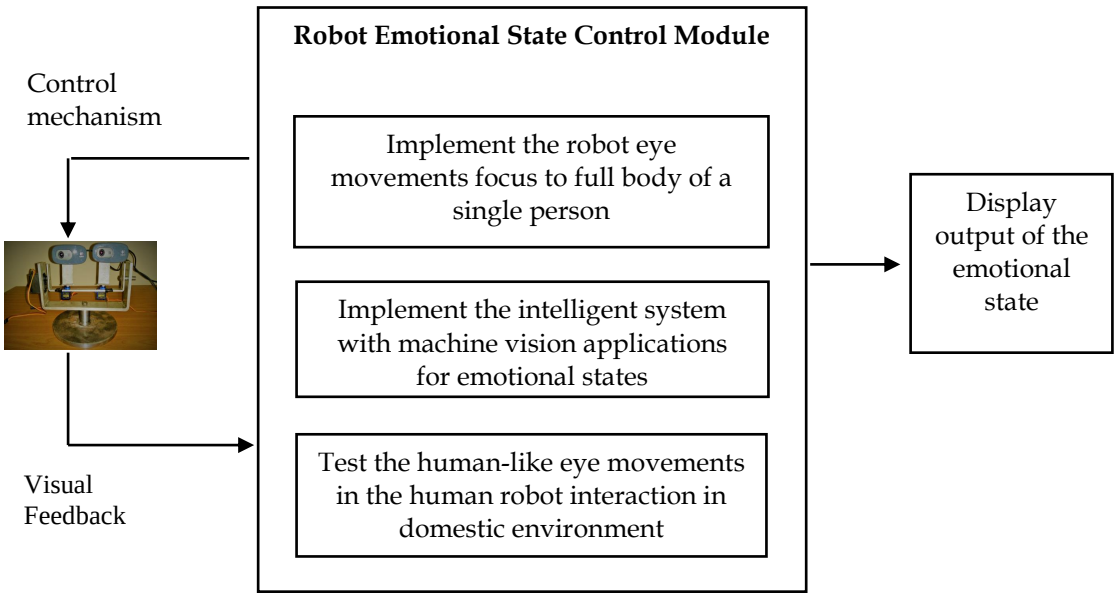

Figure 5: Implementation of intelligent system

3.2 Haar Classifier Training

The Haar Cascade classifier is used widely for object detection purposes by using images. It is developed by Viola and Jones that combined with Haar-like feature and a boosted cascade classifier. It is famous among researchers because of the higher calculating speed. Haar features can easily be scaled by increasing or decreasing the size of the pixel group that is examined. This feature allows detecting objects of various sizes (Viola and Jones, 2001). This method has been applied successfully in several object detection systems. Detect and count vehicles in traffic surveillance systems by using Haar-like feature shows above 90% accuracy for the developed system (Choudhury et al, 2017). Detect white blood cells by using haar cascade classifier shows to localize white blood cells with high precision and high recall values as 95% and 74% respectively (Budiman et al, 2016). Haar classifier training used several numbers of positive images and negative images to classify emotions. This feature allows detecting emotion in human with different body postures. The Extensible Markup Language (XML) file is the creation of classifier training which includes body postures related to emotions. Images of two persons were used to train each emotion classifier of the developed intelligent system. They are the known persons in the intelligent system. The number of positive and negative images are taken

by most of the researchers in the ratio of 1: 2 (Budiman *et al*. 2016; Ulfa and Widyantoro, 2017). Therefore 2000 of positive images and about 4500 of negative images were used to train each emotion classifier training process.

3.3 Emotion Recognition Using Intelligent System

Functional flow of the intelligent system is shown in Fig. 6. Developed robot eye model is continuing searching for a person's body posture to detect his emotional state. Always the robot eye tries to find an emotional state according to train emotion classifiers until detection of an emotional state. Therefore, the robot eye only rotates with pan till movement to detection of an emotion of the person. The values of field of view, focal length, optical resolution and frame rate are used to select a camera for the robot eye (Logitech, 2017). Each camera captures the video separately. Each resultant window has a video resolution of 640 pixels wide and 480 pixels high with 30fps maximum frame rate. First, emotions are classified according to body postures. These classifiers are created by using about 2000 images with the same body posture pattern. The regions and their events are contained within the regions of each classifier according to body postures for each emotion. This intelligent system was developed by using twelve emotional classifiers. During the implementation of the robot eye, the intelligent system checks that image pattern by using live video stream. If a trained emotion classifier detects in the intelligent system during implementation, the Region Of Interest (ROI) is chosen according to the classifier. After detecting an emotional state, the focusing algorithm always tries to get the ROI to the middle of the window by using pan and tilt movement of the robot eye. Pixel numbers of depth and width are used in the resultant window to develop that focusing algorithm.

3.4 Graphical User Interface (GUI) for Display Emotions

A GUI is used to display the emotional state of the human. It was created by using an algorithm in visual studio C++ to display four resultant windows inside in one resultant window. It comprises left robot eye, right robot eye, emotional state and feeling faces according to the emotions. According to the train classifiers, the intelligent system gives a signal to the GUI model to state the emotional state as happy, sad and relax. This given signal can be used to develop various algorithms for service robot to do separate tasks according to given signal. The emotional state with their feeling faces according to each emotion type are shown in Table 1.

Table 1: Emotional states with their feeling faces

Emotional state	Feeling face
Happy Mood	
Sad Mood	
Relax Mood	

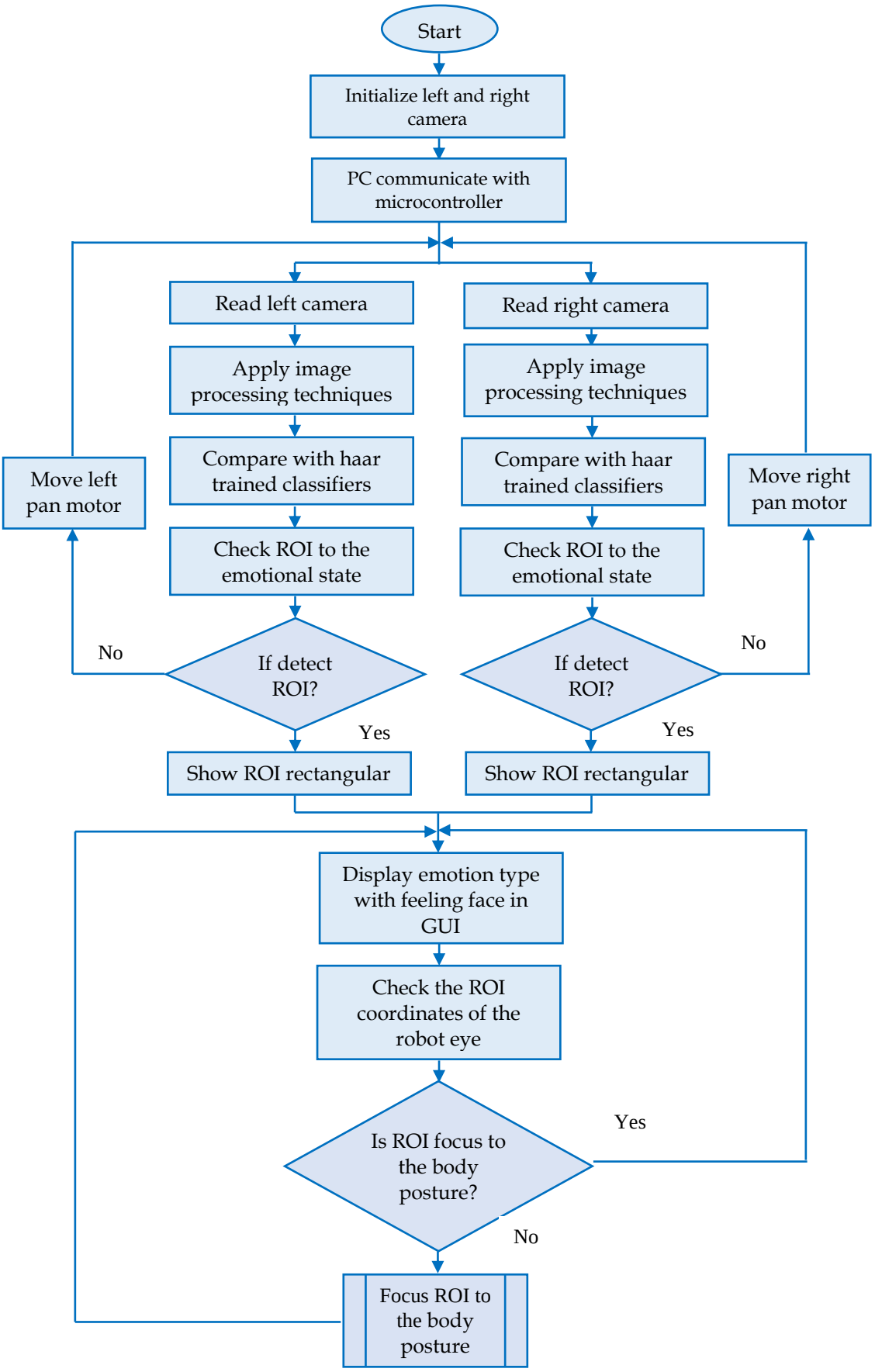

Figure 6: Functional flow of the intelligent system

4 RESULT AND DISCUSSION

4.1 Experiment Setup

The experiment conducted environment is shown in figure7. There are some unnecessary things in the environment like chairs, a table, a curtain and a flower vase. But during the implementation, the intelligent system detects and focuses only person's emotional state according to the body posture while rejecting the other things in the environment. Figure 8 shows the implementation of the robot eye.

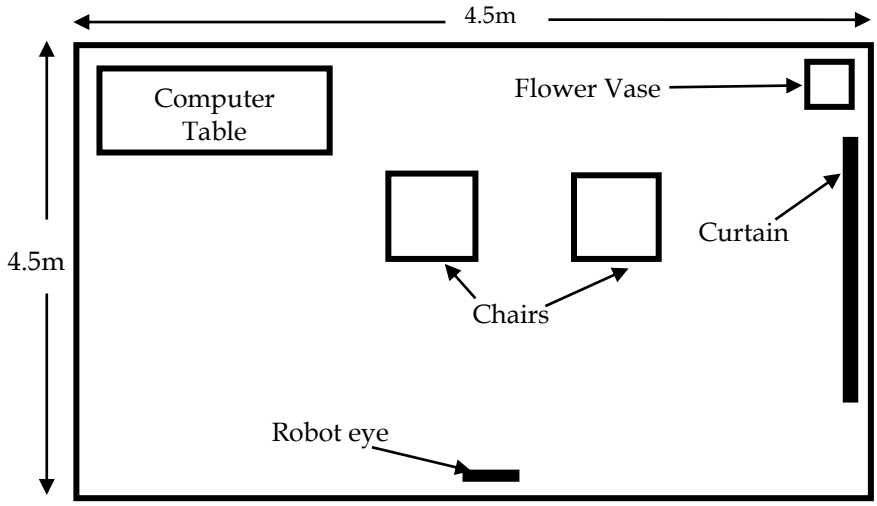

Figure 7: Domestic environment that trains intelligent system

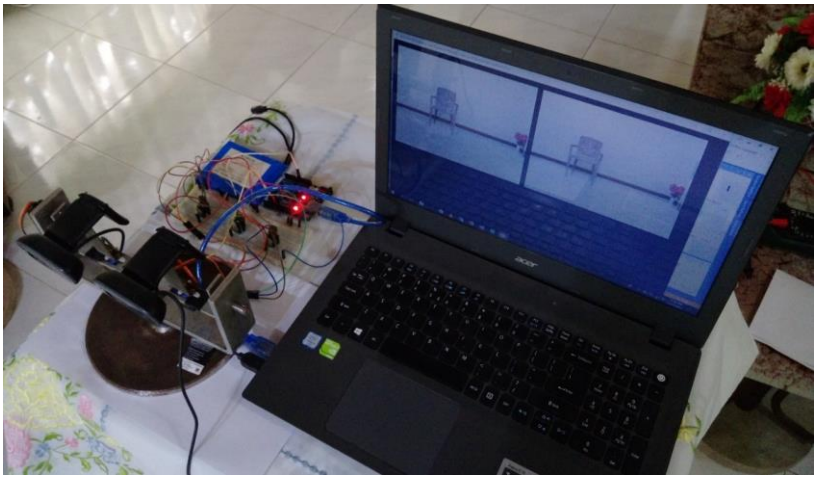

Figure 8: Implementation of the robot eye

4.2 Speed of Robot Eye Rotation

Servo motor rotation speed is an important factor which affects the behaviour of the robot eye. During the high-speed eye rotation by using servo motors, there can be some vibrations of the robot eye and missing ROI ranges during implementation due to not focusing ROI range according to body postures. It will be harmful to the robot eye visual feedback to the intelligent system. Table 2 shows the angles per each step and the rotation speed of the servo motors for those steps. As a result of this the robot eye is developed by using the slowest speed of servo motors. It also helps to detect emotional states accurately by correct focusing on the person's emotional state.

Table 2: Servo motor rotation speeds during implementation

Angles per each step	Time for rotation		Angle per second (pan axis)	Angle per second (tilt axis)
	Pan axis	Tilt axis		
1^0	8.0s	6.9s	8.75^0	8.6^0
2^0	4.0s	3.5s	17.5^0	17^0
3^0	2.6s	2.3s	26.9^0	25.4^0
4^0	2.0s	1.8s	35^0	33.2^0

4.3 Results of the Emotion Recognition

A simple experiment was conducted to ensure the success of robot eye in emotion recognition. Performed sample experiment includes two of happy emotion body postures, two of sad emotion body postures and two of relaxing emotion body postures. Three persons are selected for the experiment which includes two known persons of intelligent system and one unknown person in the intelligent system. Detection of emotions in GUI and the rotation angles during implementation is shown in Figure 9(a) to Figures 9(f).

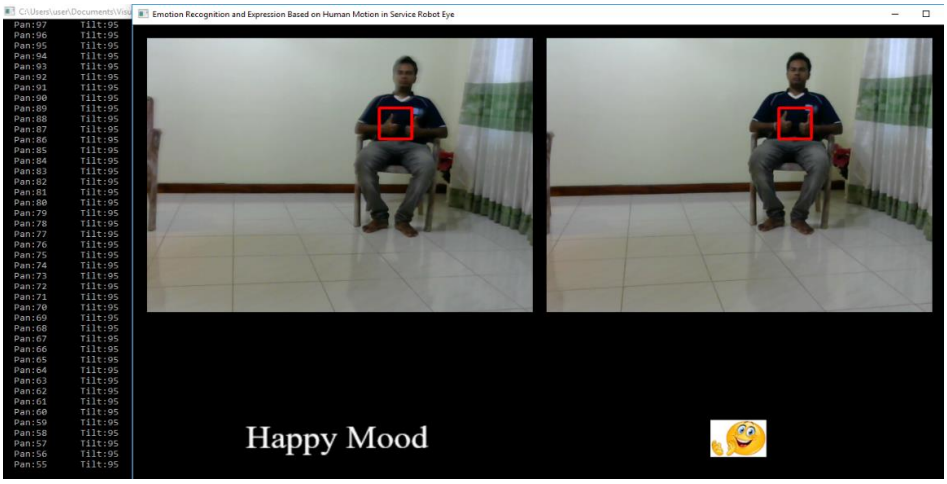

Figure 9(a): Result obtain in GUI by focusing to the Happy mood of known person 1 on intelligent system (T=4s)

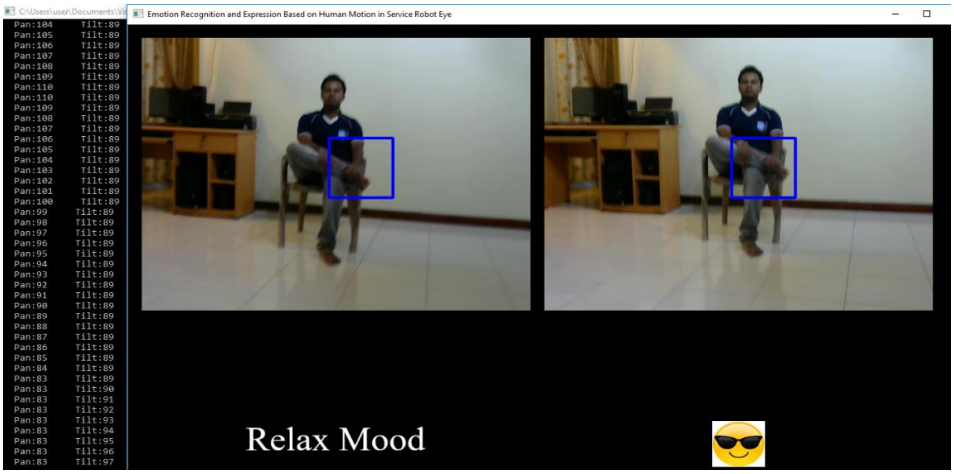

Figure 9(b): Result obtain in GUI by focusing to the Relax mood of known person 1 on intelligent system (T=13s)

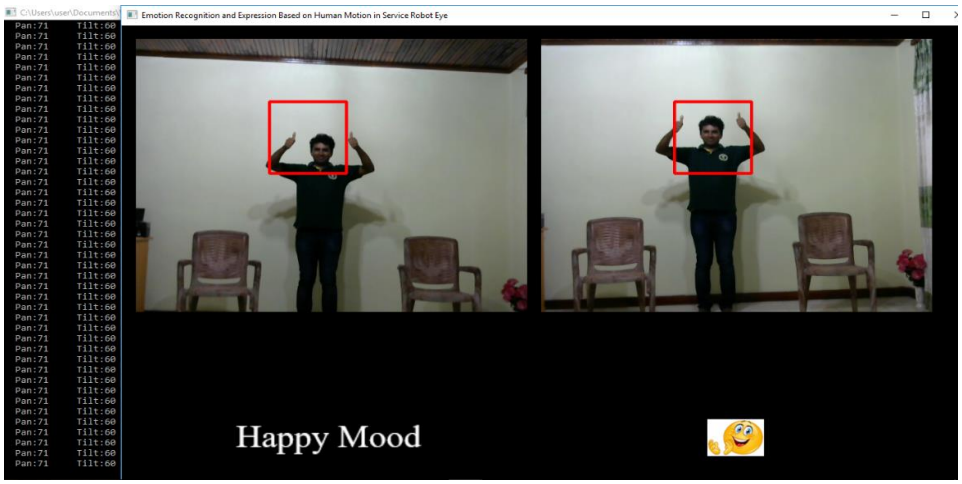

Figure 9(c): Result obtain in GUI by focusing to the Happy mood of known person 2 on intelligent system (T=21s)

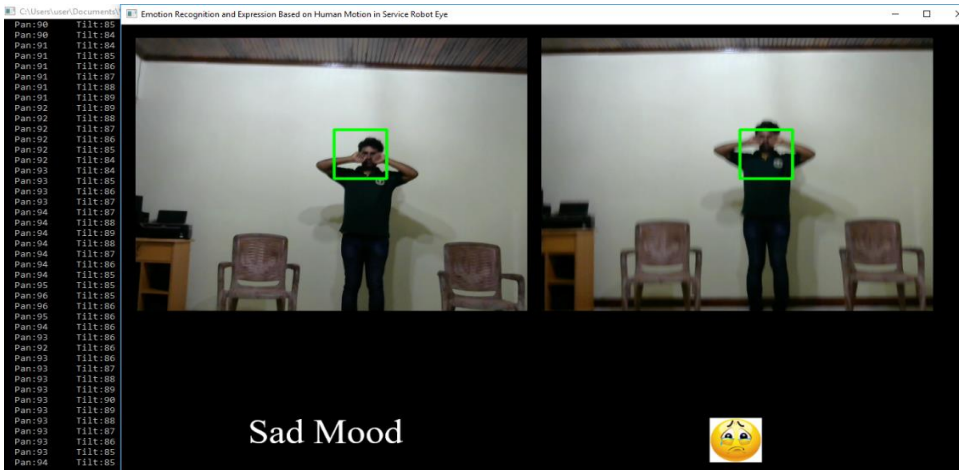

Figure 9(d): Result obtain in GUI by focusing to the Sad mood of known person 2 on intelligent system (T=31s)

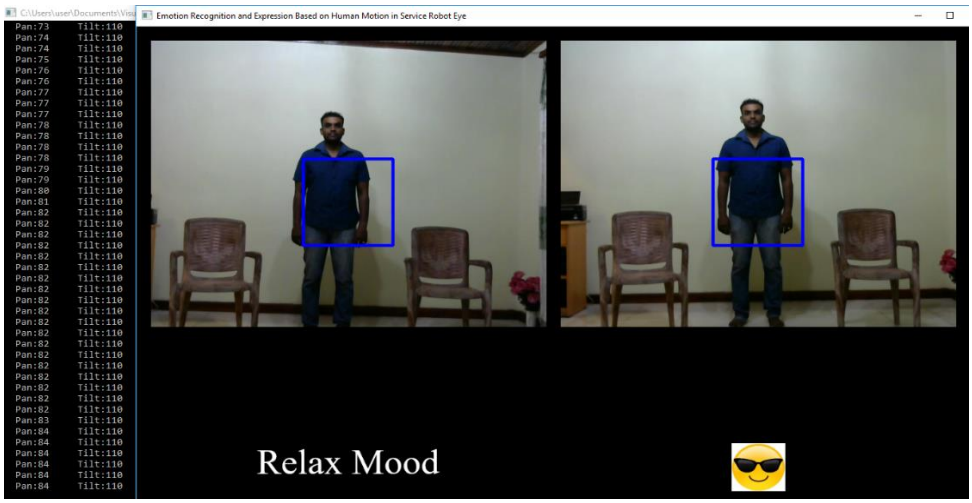

Figure 9(e): Result obtain in GUI by focusing to the relax mood of unknown person on intelligent system (T=37s)

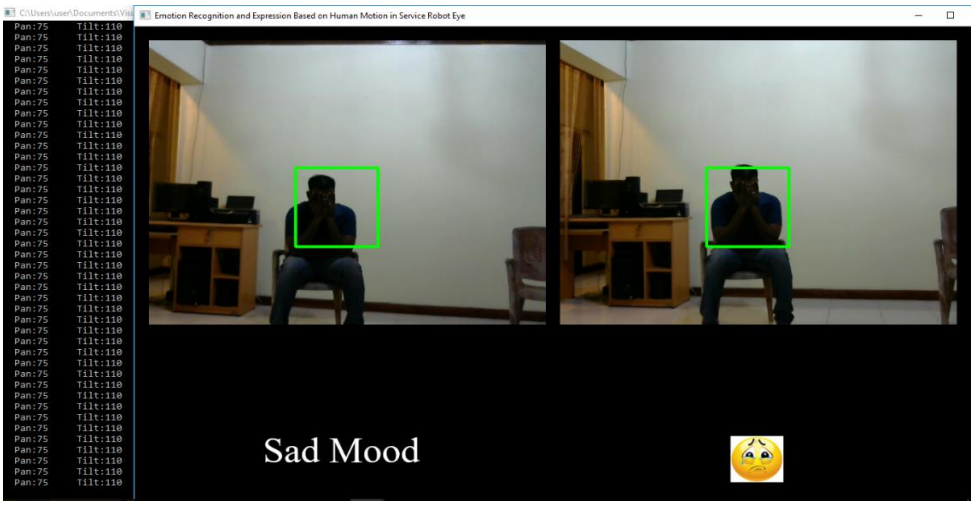

Figure 9(f): Result obtain in GUI by focusing to the sad mood of unknown person on intelligent system (T=46s)

Figure 10 shows the servo angle rotation of robot eye during implementation. This experiment was conducted in a 50s-time period. Classifiers are detected emotions only for the trained body postures. If not detect a trained classifier, then the robot eye always tries to find an emotional state. Six places have constant rotation angles in the pan motor rotation. The robot eye detects emotions of the person during that time periods and they are the time periods that body postures are similar to trained emotion classifiers. After detecting emotion type, pan and tilt motors try to focus it to the middle of the window. Therefore, the tilt motor rotation angle is also stable in each case. There are also some time period's in high gradients. It means during that time period, the robot eye is trying to find an emotional state by using the pan and tilt movement.

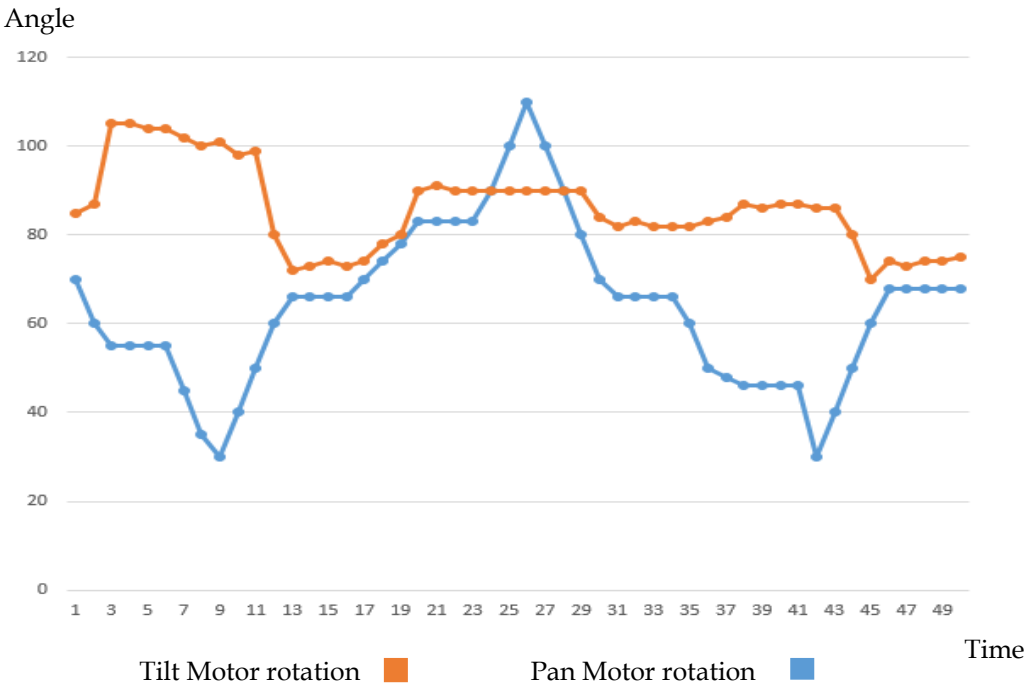

Figure 10: Servo angle rotation of the robot eye during implementation

4.4 Accuracy of the Intelligent System to Detect Human Emotion

As a result of this experiment the emotions are detected successfully. Table 3 shows the summary of experimental results with the accuracy of each classifier.

Table 3: Summary of experimental results with the accuracy of each classifier

Emotion type	Room size (m^2)	Emotion detecting distance from robot eye(m)	No. of samples taken from each person in different positions	Accuracy of system with known person-1	Accuracy of system with known person-2	Accuracy of system with unknown person-1
Relax in a chair	20.25	3.0	40	82.5%	85.0%	65.0%
Relax in standing	20.25	3.6	40	80.0%	72.5%	62.5%
Happy in a chair	20.25	3.0	40	75.0%	80.0%	70.0%
Happy in standing	20.25	3.6	40	82.5%	77.5%	65.0%
Sad in a chair	20.25	3.0	40	72.5%	77.5%	57.5%
Sad in standing	20.25	3.6	40	87.5%	82.5%	75.0%
Overall accuracy of the intelligent system for each person				80.0%	79.2%	65.8%

This experiment was done in a domestic environment. Therefore, the room size is limited to 20.25m^2. The table includes the average distances between robot eye and the person to detect emotions in each classifier. During the experiment, the person is changed for different 40 positions in the environment. Therefore, the accuracy of each classifier states separately. Finally, the overall accuracy of the intelligent system was calculated for each person. According to the results of Table 3, the trained classifier detects emotions with high accuracy for known persons in the intelligent system. The result of unknown person is lower than known persons of intelligent system. By analyzing the results during implementation, there were some places that couldn't identify emotions accurately due to the availability of some disturbance in the domestic environment. Changing light illumination of corners of the experiment conducted room and limited field of view of the robot eye are the disturbances for the intelligent system. Fig. 11 shows the result of the experiment by using the detected and undetected areas during implementation.

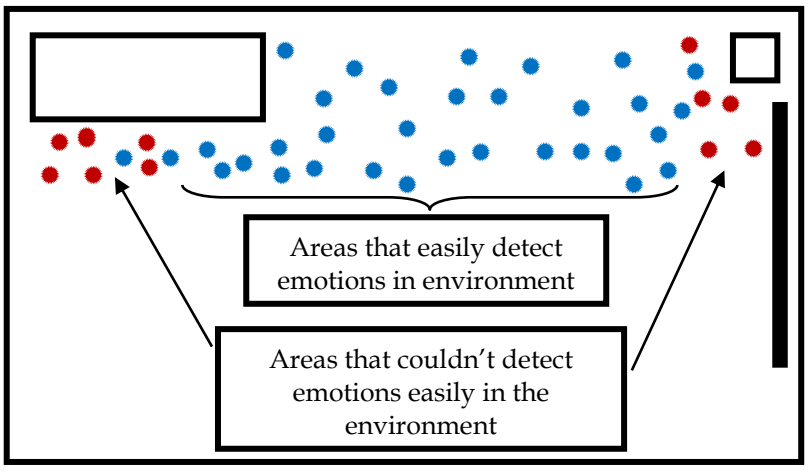

Figure 11: Areas that emotions easily detected and undetected during the experiment

The middle of the room has a wall with white background. Therefore, a weak classifier also can detect emotions easily from using those areas in the intelligent system. But in corners of the room resist recognizing emotions from the weak classifier due to disturbances that shown above, but the emotions are detected with low accuracy in those areas. Each classifier in the intelligent system is trained by using about 2000 positive images and 4500 negative images. This experiment was done by using three persons. Two of them are known persons of the intelligent system and one person is an unknown person in the intelligent system. A strong classifier can be made by using more images by using different light illuminations and images of different persons to get a maximum result from the intelligent system.

5 CONCLUSION

The robot eye is designed for service robots to replace caregiver. As the first step of human-robot interaction, it must identify the emotional states of the human. After the recognition of emotion, algorithms can be developed to the interaction part of the service robot. Therefore, robot eye development is an important factor in service robot designing. There are some factors to be considered to increase the accuracy of the developed system during designing, tracking and focusing robot eye. They are camera selection, actuators selection, material selection for the robot eye design and software selection to develop the intelligent system. Each haar classifier training spends about 4 hours to train each experimental classifier. It depends on the data set which provides to the classifiers. Light illumination is a factor in classifier training. If the lighting condition change during capture images to haar training process, the data set should have more images to train a successful emotion classifier and it also spends more than four hours. Therefore, the maximum accuracy of the robot eye can be obtained only in a domestic environment where the intelligent system was trained. Emotion types are trained by using two people's images in the intelligent system. A strong classifier can make from using different person images with different colour illumination backgrounds. It also increases the classifier accuracy. Then the robot eye can be used for any domestic environment to detect emotions of the human successfully. The designed robot eye has been tested for different test cases by changing the emotional states of the person. From this test, scenarios can conclude that the haar classifier training algorithm is superior to other algorithms in order to track and search the position of the respective emotions according to body postures of elders and disables. The system can be developed by adding more images to haar classifier training process to make strong classifiers.

The proposed robotic eye is designed in such a way that it can be used as a platform for facilitating further developments in integrating more interactive features to the robotic eye. The robot eye could significantly improve with redesigning. After trials with robot eye for service robot to determine whether it is feasible to use the robot for its intended purpose, the overall design, materials and manufacturing techniques should be evaluated and optimized for the number of robots that are expected to be made. Designed robot eye model size is not equal to the human eye. By using a proper design, the outward appearance of the robot eye also can be improved to equal for human eyes. A proper outer cover helps to enhance the appearance of the robot eye. It is better to design an outer cover using molding techniques with low weight materials. The robot eye will interact well if it has more sensors in robot eye design. Therefore, the research project has further developments. The robotic eye can be used as a research platform for implementing various control strategies such as artificial intelligence systems and machine learning techniques to smooth the emotion recognition process as more human-like manner.

6 ACKNOWLEDGEMENT

The author would like to acknowledge Mr. B.G.D.A Madhusanka, Mr. HDNS Priyankara, Mr. W.R. De Mel and Mr. W. A. R. Nandana for giving me their support and assistance throughout this work.

REFERENCES

1 Ceccarelli, M. (2012). Service Robots and Robotics: Design and Application, Italy: IGI Global, pp. 1.

2 Lamberti, F. Paravati, G. and Salvo, A. (2016). Service Robotics [online]. Available at: https://www.computer.org/web/computingnow/archive/service-robots-october-2016. [Accessed 13th May 2017].

3 Suryadevara, K. and Mukhopadhyay, C. (2015). Smart homes design, implementation and issues: springer international publishing Swisterland, pp.12-15.

4 Sirithunge, C., Chandima, P., Muthugala, J., Buddhika, G. and Jayasekara, P. (2017). Interpretation of interaction demanding of a user based on nonverbal behavior in a domestic environment, *IEEE International Conference on Fuzzy Systems*, pp. 1-8.

5 Tosa, N. and Nakatsu, R. (1996). Life-like communication agent - emotion sensing character "MIC" and feeling session character "MUSE"", *3rd IEEE International Conference on Multimedia Computing and Systems*, pp.12-19.

6 Dammak, M., Ammar, B. and Alimi, M. (2012). Real-time analysis of non-verbal upper-body expressive gestures, *IEEE International Conference on Multimedia Computing and Systems*, pp. 334-339.

7 Wickramaratne, D., Buddhika, G. and Jayasekara, P. (2017). Attention level approximation of a conversation in human-robot vocal interaction using prosodic features of speech, *IEEE Moratuwa Engineering Research Conference*, pp.40-45.

8 Laranjeira, A., Frazão, X. Pimentel, A. and Ribeiro, B. (2016). How Deep Can We Rely on Emotion Recognition, *CIARP: Progress in Pattern Recognition, Image Analysis, Computer Vision, and Applications*, pp 511-520.

9 Han, F. (2017). A Modern Course in University Physics: Optics, Thermal Physics, Modern Physics, China, world scientific publishing Co. Pvt. Ltd, pp. 48-52.

10 Maes, P., Mataric, J., Meyer, A., Pollack, J. and Wilson, W. (1996). Orientation Behavior Using Registered Topographic Maps, *From Animals to Animats 4, Proceedings of the Fourth International Conference on Simulation of Adaptive Behavior*, pp. 94-103.

11 Hayhoe, M., Gillam, B., Chajka, K., and Vecellio, E. (2009). Visual Neuroscience: Cambridge University, USA, pp. 73-80.

12 Logitech. (2017). Specifications [online]. Available at: http:// support. logitech.com/en_us/product/hd-webcam-c270/specs [Accessed 2nd September. 2017]

13 Komogortsev, O., Karpov, A., Price, L. and Aragon, C. (2012). Biometric authentication via oculomotor plant characteristics, *5th IAPR International Conference on Biometrics,* pp. 413 – 420.

14 Viola, P. and Jones, M. (2001). Rapid object detection using a boosted cascade of simple features, *IEEE international conference on Computer Vision and Pattern Recognition*, pp. 511-518'

15 Choudhury, S., Chattopadhyay, S. and Hazra, T. (2017). Vehicle detection and counting using haar feature-based classifier, *8th IEEE international conference on Industrial automation and electromechanical engineering*, pp.106-109.

16 Budiman, R., Achmad, B., Faridah., Arif, A., Nopriadi and Zharif., L. (2016). Localization of White Blood Cell Images using Haar Cascade Classifiers, *1st IEEE international conference on biomedical engineering*, pp. 1-5, 2016.

17 Ulfa. D. and Widyantoro. D. (2017). Implementation of haar cascade classifier for motorcycle detection, *IEEE International Conference on Cybernetics and Computational Intelligence*, pp.39-44, 2017.

Bluetooth Low Energy Local Positioning for Museum Navigation

N.D.C.D. Kannangara, W.D.S.S. Bandara*

Department of Electrical and Computer of Engineering, The Open University of Sri Lanka, Nawala, Nugegoda, Sri Lanka.

*Corresponding Author: email: wdban@ou.ac.lk, Tele: +948774674793

Abstract – *Bluetooth Low Energy (BLE) is a new specification of Bluetooth available for all new smart-devices. It is a new low power consumption technology aimed to transmit small amount of data. In addition to the transmitting data, BLE can be used to locate objects. iBeacon® protocol, which uses BLE, is aimed at that objective with special attention in proximity location with BLE beacons. This is a new technology and as yet it is unclear how it will be used. In conventional museums, information or explanation of exhibited artifacts is presented by using panels or leaflets. Some museums are complicated places to navigate within. They may not have a clear path through the museum and may offer many alternatives. The problem is even complicated, given the fact that a visitor usually has limited time for a visit and missed some important places. However, such paper maps may be inconvenient and not easy to use, especially when a group of visitors is visiting the museum together. The objective of this project was to implement an Android application(app) "Museum Navigation System" based on Bluetooth Low Energy beacons and the iBeacon® protocol. Here the Android app illustrates navigation and information on the smart device by using received signal strength indicator(RSSI)power, universally unique identifier (UUID), major and minor of beacon frame. Here 3 Beacons were used in a cluster to find the position. First scanned for beacons and then RSSI power values are saved in an array. Then it selects 3 most strong beacons by sorting values of RSSI power. RSSI-based triangulation method is used to find the position in a cluster and when the user moves to the next cluster region it is identified by scanning the route. Then, user position coordinate and direction on the map were displayed by app.*

Keywords*: Bluetooth Low Energy, BLE proximity location, iBeacon protocol, 3 Beacons cluster, triangulation.*

1 INTRODUCTION

One of the main objectives of a "Museum" is to provide visitors a chance to learn. In conventional museums, information or explanation of exhibited materials is presented by using panels or leaflets. Some museums are complicated places to navigate within. They may not have a clear path through the museum and may offer many alternatives. The problem is even complicated given the fact that a visitor usually has a limited time for a visit and may miss some important places. The classic navigation aid is the paper map of the museum, which is based on the museum floor plan and enables the visitor to orient themselves and find the way in the museum. However, such paper maps may be inconvenient and complicated to use, especially when a group of visitors is visiting the museum together. Current mobile technology opens new possibilities for supporting indoor navigation. Compared to classic Bluetooth, Bluetooth Low Energy consumes much

less power (e.g. 0.01 W instead of 1W), the BLE devices are considerably cheaper to build, while the data transfer rate is much lower (e.g. 0.27 Mbit/s). Meanwhile the power consumption must be low and the data rate is not important to transmit context based information to smart device such as iPhone and iPad. Beacons are small wireless sensors that communicate with Bluetooth-enabled smart devices such as iPhones or iPads by continuously advertising their location using a Bluetooth low energy radio transmitter. In turn, smart devices monitor the received signal strength indication (RSSI) and determine the device's proximity to the beacon. This is a new technology and as yet it is unclear how it will be used. Therefore, aim of the project is to develop a museum navigation system to be used in museums.

2 PROJECT BACKGROUND

2.1 Museum Navigation Systems

Similar museum navigation systems can be found in two technologies.

Museum Navigation System using Augmented Reality Technologies — Noboru Koshizuka

Tokyo University Digital Museum, has started developing a new information-providing system for exhibited materials by using "augmented reality" technologies in the computer science field. Augmented reality technologies realize some kinds of un-natural and artificial images in the real world. In other words, augmented reality technologies build unrealistic images in real world, while the virtual reality technologies build realistic images in virtual world. In this system, a visitor wears a "glass", called as Head Mounted Display (HMD). The visitor can see real images through this "glass", and the "glass" contains an LCD screen in front of the user's eyes, which can display information from a computer over the real images. Wandering around the museum wearing the "glass", the visitor can see explanation and/or information of exhibit in front of his/her eyes. If he/she puts earphones in his/her ears, he/she can listen to aural information at the same time. Approaching exhibited materials, the display will switch to more detailed explanation of the materials.

Personalized Digital Museum Assistant — Ken Sakamura

Personalized digital museum assistant (PDMA) is a tool that uses computer technology to strengthen "exhibitions" which enable visitors to achieve more enjoyment as well as greater knowledge and excitement from museums. PDMA is a term created to encompass the meaning of a tool to enjoy the personalized digital museum by using a personal digital assistant (PDA) which is the mobile terminal. A variety of formats were devised in the course of achieving the PDMA, and at the University Museum the University of Tokyo a number of formats of PDMA were researched and developed, and subjected to repeated trial testing. In principle, electronic tags are attached to exhibits, and the PDMA reads off data from the electronic tags, thereby detecting what visitors want to know about what exhibits. In response, the PDMA displays or provides a voice commentary about information related to that exhibit. The key feature of PDMA is the ability to personalize. By setting the services required by visitors when the PDMA is lent out, a commentary that meets the needs of the individual is provided. This may include aspects such as the

language used, the size of the font, the degree of specialized knowledge, and being for children, etc.

2.2 Beacons Structure and Other Beacon Applications

Beacon is a small computer. Its 32-bit ARM® Cortex CPU is accompanied by an accelerometer, temperature sensor, and most importantly 2.4 GHz radio using Bluetooth 4.0 Smart, which is also known as BLE or Bluetooth Low Energy. Beacon other applications are retail, stadium and air-port navigation systems. But those applications are still in trail condition.

3 CONCEPTUAL DESIGN

Museum Navigation System is an android application which illustrates navigation and information on the smart device by using beacons. Received Signal Strength Indicator (RSSI) power, Universally Unique Identifier (UUID), major and minor of beacon frame are used to describe the power of a beacon's signal.

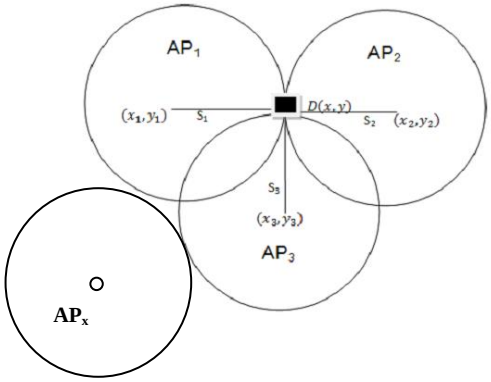

Figure 1: Cluster plan

Figure 1 shows the cluster plan with beacons and they behave as access points (APs). Here three beacon clusters are used to find the position. First beacon signals are scanned and then RSSI power values are saved in an array. After that, it selects three beacons with highest value of RSSI power. RSSI-based triangulation method is used to find the position in a cluster and when the user moves to the next cluster region it identified by scanning the route. Then it uses the identified new beacon and previous beacon to find the new position in the new region. Scan runs within constant time and updates the beacons initial position with user position on the map.

3.1 Bluetooth RSSI vs. Distance

Anti et al. presented the design and implementation of a Bluetooth Local Positioning Application (BLPA) in which the Bluetooth received signal power level is converted to distance estimate according to a simple propagation model as follows and the RSSI in dB is given by

$$RSSI = P_{TX} + G_{TX} + G_{RX} + 20\,log\,(4\pi fc) - 10n\,log\,(d) \quad (1)$$

$$= P_{TX} + G - 40.2 - 10n\,log\,(d) \quad (2)$$

Where P_{TX} is the transmit power; G_{TX} and G_{RX} are the antenna gains and G is the total antenna gain: $G = G_{TX} + G_{RX}$, c is the speed of light ($3.0 \times 10^8 m/s$), f is the central frequency ($2.44\,GHz$), n is the attenuation factor (2 in free space), and d is the distance between transmitter and receiver (in m). d is therefore:

$$d = 10^{[(P_{TX} - 40.2 - RSSI + G)/10n]} \quad (3)$$

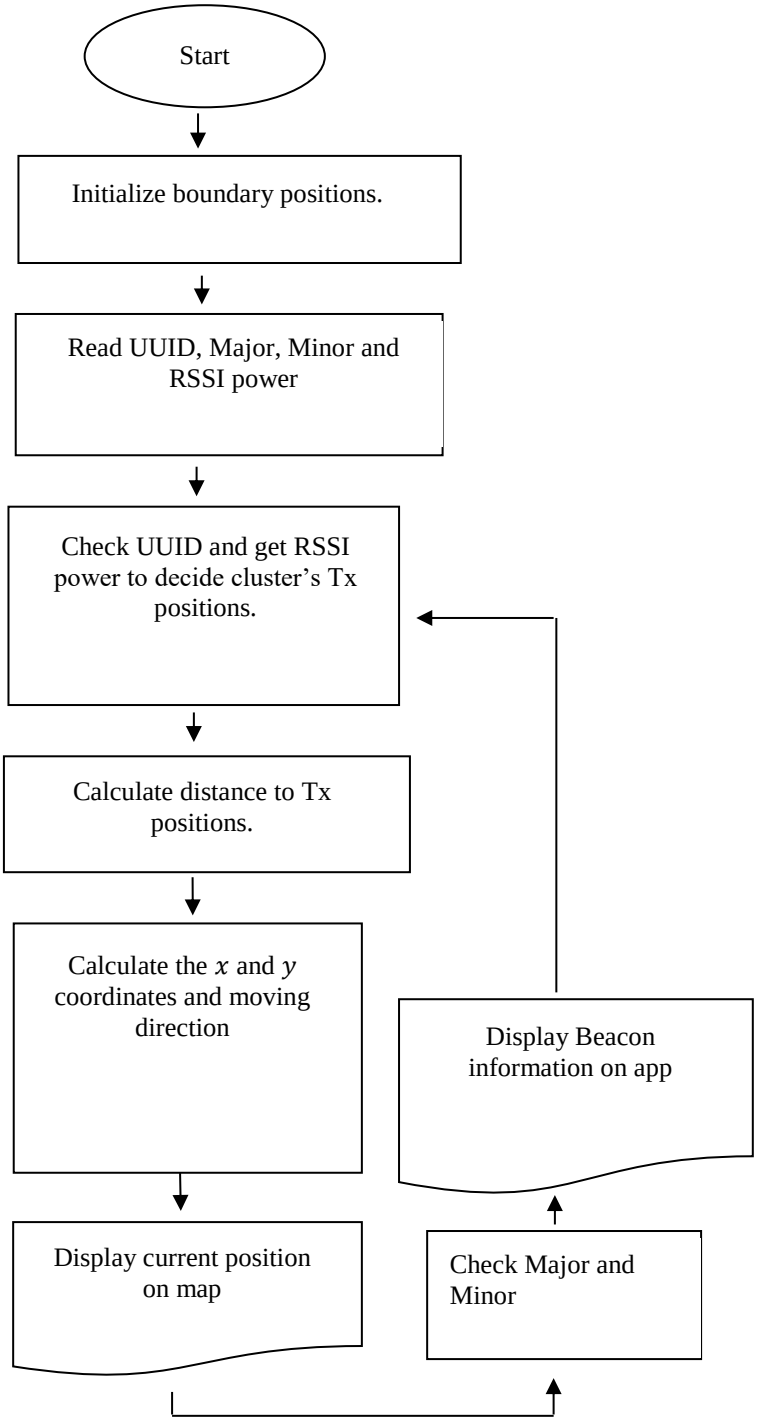

Figure 2: Flow Chart

However, such a model can only be utilized as a theoretical reference. Due to reflection, obstacles, noise and antenna orientation, the relationship between RSSI and distance becomes more complicated. Further it influences on Bluetooth RSSI values. Therefore, several experiments were carried out to understand how the Bluetooth indicators fade with distance under these environmental influences.

Let $A = P_{TX} + G - 40.2$ (4)

Therefore,

$RSSI = -10n\ log\ (d) + A$ (5)

where A is the received $RSSI$ power at $1m$

3.2 Beacon Navigation Algorithms

The algorithm is based on three beacons which can communicate with a smart device and those Beacons measures the signal coming from smart device.

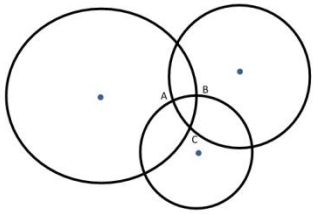

Figure 3: Measuring the signal

Let beacons coordinates be $A \equiv (x_1,\ y_1)$, $B \equiv (x_2,\ y_2)$ and $C \equiv (x_3,\ y_3)$

Then,

$x^2 + y^2 - 2x_i x - 2y_i y + y_i^2 + x_i^2 = r_i^2$ (6)

Where r_i is represented as: $r_i = 10^{[A_i - RSSI_i] / 10n}$;$i \in \{1,2,3\}$

Solving (1) – (2) and (2) – (3), the above equations reduced to two equations as:

$2(x_2 - x_1)x + 2(y_2 - y_1)y = r_1^2 - r_2^2 - x_1^2 + x_2^2 - y_1^2 + y_2^2$ (7)

$2(x_3 - x_2)x + 2(y_3 - y_2)y = r_2^2 - r_3^2 - x_2^2 + x_3^2 - y_2^2 + y_3^2$ (8)

Let us define: $a = 2(x_2 - x_1), b = 2(y_2 - y_1), c = 2(x_3 - x_2), d = 2(y_3 - y_2),$

$e = r_1^2 - r_2^2 - x_1^2 + x_2^2 - y_1^2 + y_2^2$ and $f = r_2^2 - r_3^2 - x_2^2 + x_3^2 - y_2^2 + y_3^2$

Then,

$$ax + by = e \tag{9}$$

$$cx + dy = f \tag{10}$$

Finally, the coordinate of the device being tracked is:

$$x = \frac{de-bf}{ad-bc} \ , \qquad y = \frac{ce-af}{bc-ad} \tag{11}$$

Here $ad = bc$ case appears when $(x_2 - x_1)(y_3 - y_2) = (x_3 - x_2)(y_2 - y_1)$ and it occurs when the beacons are only overlapped. But practically no two beacons are overlapped. The actual motion is the most important things to improve model's accuracy. In this case higher order equations are used to determine the distance that user moves in time period (here able to use scanned time duration).

$$S_x = U_x t + \frac{A_x}{2} t^2 + \frac{B_x}{6} t^3 + \frac{C_x}{24} t^4 + \ ... \tag{12}$$

$$S_y = U_y t + \frac{A_y}{2} t^2 + \frac{B_y}{6} t^3 + \frac{C_y}{24} t^4 + \ ... \tag{13}$$

For the velocity

$$U_x = \frac{(x - x')}{t} \ , \qquad U_y = \frac{(y - y')}{t} \tag{14}$$

For the acceleration

$$A_x = \frac{(U_x - U_x')}{t} \ , \qquad A_y = \frac{(U_y - U_y')}{t} \tag{15}$$

For the rate of change of acceleration or jerk

$$B_x = \frac{(A_x - A_x')}{t} \ , \qquad B_y = \frac{(A_y - A_y')}{t} \tag{16}$$

Assume all the beacons transmit same signal power and average of velocity, acceleration etc. can be obtained. Therefore, by substituting equation 9 and 10 to 11 and 12 then A_i, B_i related to x_i and y_i are calculated. Then the values of S_i which are related to x_i and y_i are finally calculated and the position of x and y. Every dash (') values are previous values and t is scan time.

Error of the motion and distance ~ $Ct^4/24$

$$X_{current} = X_{previous} + S_x \tag{17}$$

$$Y_{current} = Y_{previous} + S_y \quad (18)$$

Then here used pointer rotation to indicate user moving direction by using current and previous coordinates.

$$\theta = \tan^{-1}\left(\frac{y_{current} - y_{previous}}{x_{current} - x_{previous}}\right) \quad (19)$$

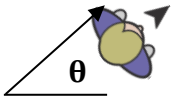

Figure 4: Direction of pointer

3.3 Error Calculation

Root mean square error is used to find the error between actual point and calculated point. It is a frequently used as the measure of the differences between values predicted by a model or an estimator and the values observed. It represents the sample standard deviation of the differences between predicted values and observed values.

$$\text{Root Mean Square Error} = \frac{1}{N}\sum_{i=1}^{N}\sqrt{(x_{true} - x_{final,i})^2 + (y_{true} - y_{final,i})^2}$$

4 PROPOSED METHODOLOGY

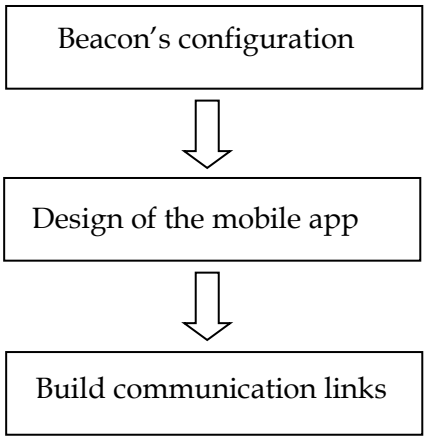

Figure 5: Project steps

4.1 Beacon's Configuration

Beacons broadcast in regular intervals (e.g. something between 100ms and 1 second) and can paired with neighbouring Bluetooth devices by sending out their ID. The ID consists of three parts, they are UUID (organization or company), Major (arbitrarily, e.g. specific museum) and Minor (e.g. location in museum). For example, UUID will be the same for the whole museum, while the major number can identify a large group (King's jewellery), and the minor number can identify a specific beacon for a specific object (crown).

4.2 Communication Links

Beacon frames are transmitted by the Access Point (AP) in an Infrastructure Basic Service Set (IBSS). The android platform includes support for the Bluetooth network stack, which allows a device to wirelessly exchange data with other Bluetooth devices. The application framework provides access to the Bluetooth functionality through the Android Bluetooth APIs. These APIs let applications wirelessly connect to other Bluetooth devices, enabling point-to-point and multipoint wireless communication. Using the Bluetooth APIs, an Android application can establish radio frequency channels, connect to other devices through service discovery, transfer data to and from other devices and manage multiple connections.

4.3 BLE interference with Wi-Fi

The BLE physical layer divides the 2.4GHz ISM band into 40 channels. Three of them are dedicated for advertising (finding and connecting other devices). These channels are located between the commonly-used Wi-Fi channels 1, 6, and 11, with the idea that these frequencies will be free of interference. (Wi-Fi bandwidth is 20MHz, but the channel spacing 5MHz, making 1, 6, and 11 the only set of three channels with no overlap.) The remaining 37 channels are for data. The frequency hopping algorithm simply increments the channel number by a hop value every transmission. Since the number of data channels is a primer, all channels get an equal chance.

4.4 Interference with Mobile

When the received data packet contains UUID, Major, Minor and Tx Power, it is detected as a beacon by the Android application and otherwise omit the data.

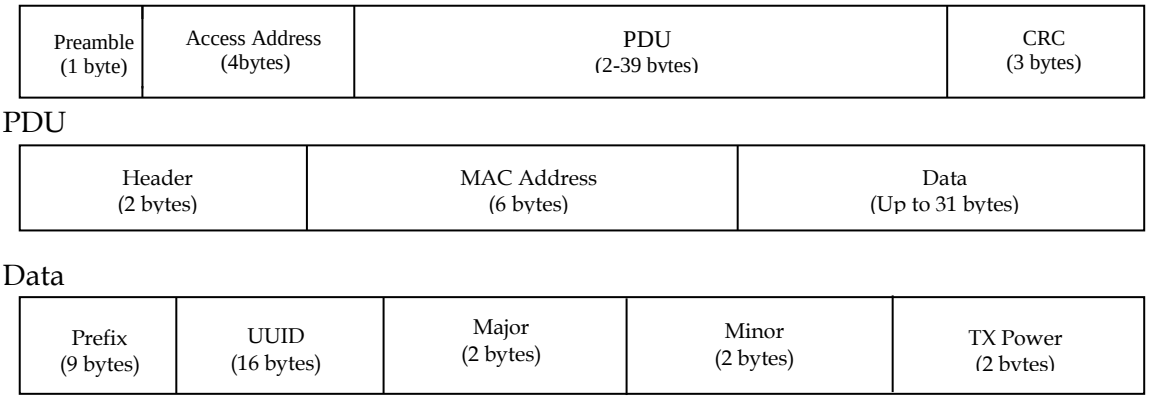

Figure 6: BLE packet structure and beacon data structure

5 IMPLEMENTATION

At this point, all necessary concepts related to indoor navigation have been explained. Information about the technologies used in this project as well to use them in positioning algorithms has been also covered. In this section all this information is put together and implemented into a navigation system consisting a group of beacons and an Android application. The system works as follows: first, few beacons are positioned around an area. Then the application scans for them and gathers their RSSI readings. These readings are, in turn, used to calculate the distance between the user and each beacon. Since no information being broadcasted by the beacons indicates their position relative to the receiver, the application makes use of calculated x and y coordinates to indicate direction of the user is moving. Both the beacons' and the user's position, as well as the distance between them, are shown in a map.

5.1 Testing Environment

The system was tested inside a 30 m^2 apartment where three beacons, separated by approximately 5 m, were placed. The map of the apartment as well as the placement of the beacons is shown in figure. The reason for setting this kind of testing environment is to test the accuracy of the system based on its capability to calculate the distance from beacons that are positioned close to each other. This situation will give an idea of how beacons should be configured regarding their output power, which will affect the range they can achieve and the RSSI readings collected by the application. For example, if the area is no more than 100 m^2 there is no point using several beacons operating with an output power of 0 dBm (around 50 m range). This will only cause the beacons to consume unnecessary power and affect the accuracy of the distance calculations as RSSI values will barely change.

5.2 The Application

At the start, a dialog is displayed on the screen asking permission from the user to turn on the Bluetooth adapter. Once this dialog is cleared, the application immediately starts scanning for beacons.

5.3 Scanning

The BLE adapter scans for nearby BLE devices and the results of the highest three RSSI power in every scan are passed through an algorithm of positioning. Then from that previous and current values direction of moving is calculated and displayed on the map. During that time, context based data captured by using major and minor values are also indicated on the display.

5.4 User's Movement

Note that the application knows how far the user is from each of the beacons, it can also estimate its position and display it in the map. This is done by displaying a black arrow with man, referred to as "pointer", representing the user and moving it through the screen as the user walks around the navigation area. In order to calculate the user's initial location, distance calculations to the closest beacons are selected and used to position the pointer as

accurately as possible within the map. However, the pointer is located relatively to the configured beacons as shown in Figure 6. It is also important to have in mind that the pointer is only used to roughly show the user's position and might not be always 100% precise. Considering the accuracy of the distance calculations, the pointer may not behave as expected and might appear closer or further from the actual position of the beacon. This inaccuracy may be tolerated as long as the position shown is not too far from reality and the user can have an idea of where he/she is.

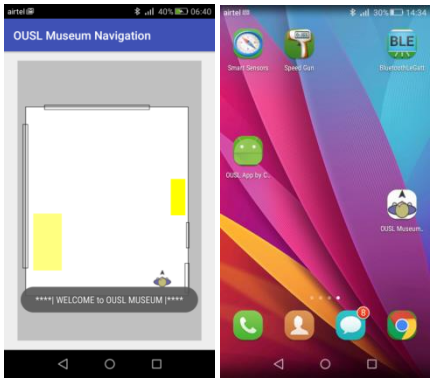

Figure 7: Screen prints of navigation app

6 SIMULATION RESULTS

A test Android application is used to measure RSSI power at given distances. Figure 8 shows the RSSI power values by changing the beacons and observing for 20 samples.

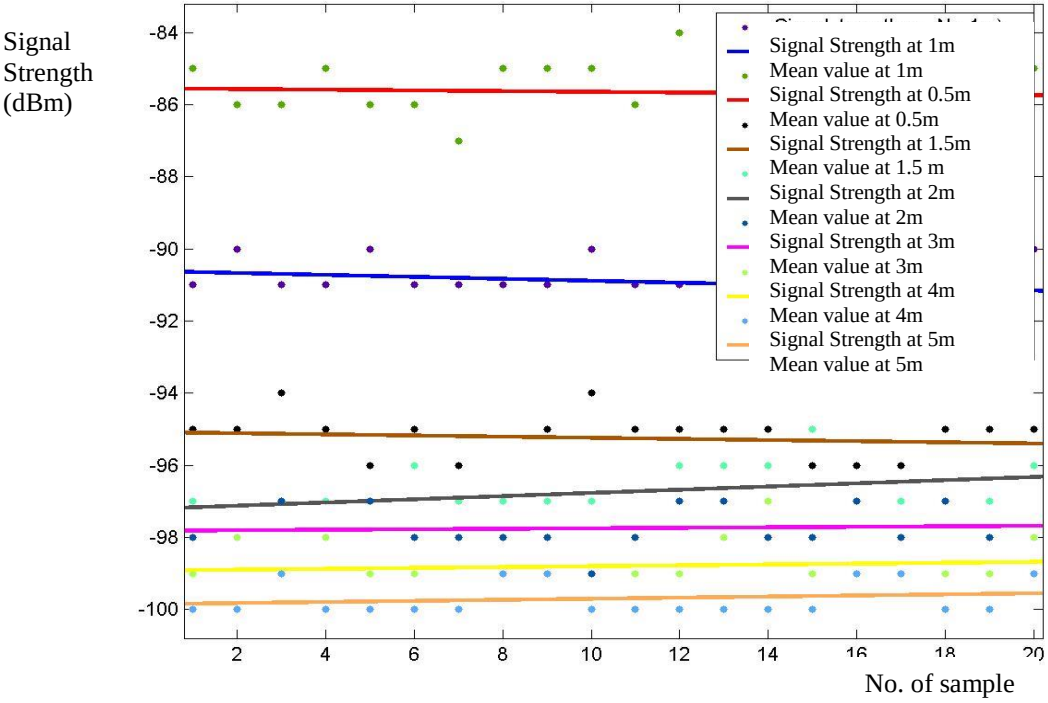

Figure 8: RSSI Power Vs Distance

Linear model Poly1: $F(x) = p_1 x + p_2$

Table 1: Static result for data

Distance	Coefficients (with 95% confidence bounds):		Goodness of fit:			
(m)	P1	P2	SSE:	R-square	Adjusted R-square:	RMSE
0.5	-0.0097(-0.072, 0.0524)	-85.55(-86.3, -84.8)	10.49	0.006022	-0.0492	0.7633
1	-0.027 (-0.092, 0.037)	-90.62(-91.4, -89.84)	11.31	0.04129	-0.01197	0.7928
1.5	-0.015 (-0.075, 0.0436)	-95.08(-95.1, -94.37)	9.584	0.017	-0.03761	0.7297
2	0.044 (-0.0114, 0.1002)	-97.22(-97.8, -96.55)	8.441	0.1342	0.08612	0.6848
3	0.0067 (-0.039, 0.0527)	-97.82(-98.3, -97.27)	5.72	0.005296	-0.04997	0.5637
4	0.012 (-0.045, 0.069)	-98.93(-99.6, -98.23)	9.104	0.01046	-0.04451	0.7112
5	0.01504(-0.024, 0.054)	-99.86(-100, -99.39)	4.05	0.0358	-0.01776	0.4743

The above table shows the coefficients p_1 and p_2 of linear the linear models with considering 95% confidence bound.

6.1 Decision for Obtaining Value of RSSI Power at 1m

Here, it is very important to get "A" value for logarithm function.

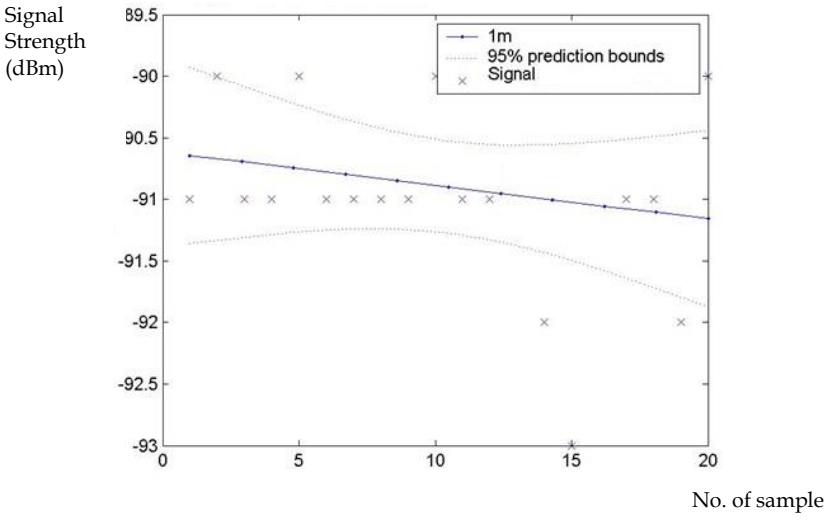

Figure 9: Analysis of fit 1m for data set

Therefore,

$$RSSI = -10n\,log\,(d) + A$$

$$= -10n\,log\,(d) - 91$$

From the above data, n = 1.5; which is the attenuation constant and it is depend on the environment.

6.2 Simulation Results

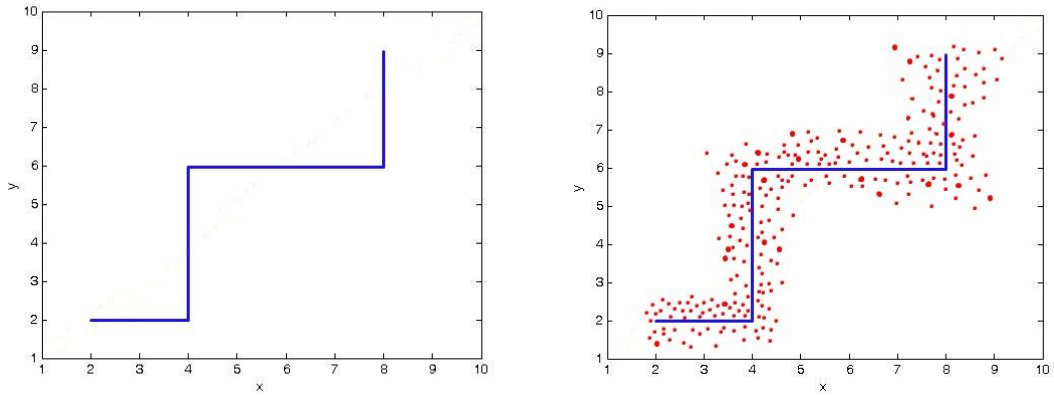

Figure 10: Actual path of smart device and points measured by smart device

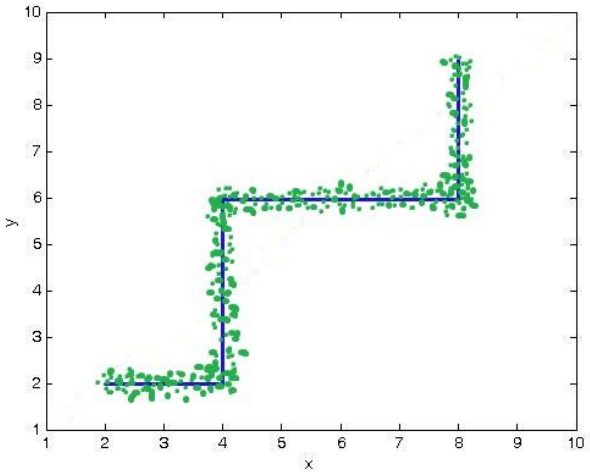

Figure 11: Final points

6.3 Product Test Results

Product was tested at research laboratory in the department of Electrical and Computer Engineering of the Open University of Sri Lanka.

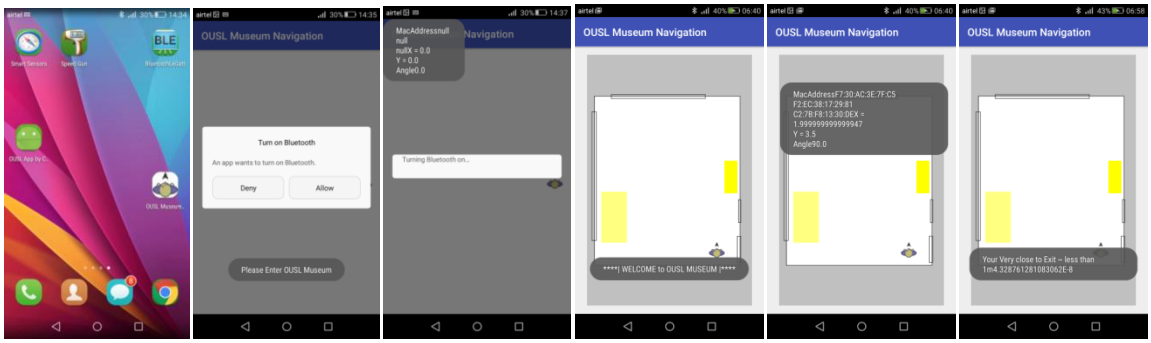

Figure 12: Screen prints of product test

7 CONCLUSION

As opposed to the well-established concept of outdoor navigation, indoor navigation must still overcome many challenges before becoming an everyday use commodity. One example is the limited amount of technologies that can be used for this purpose, as well as the accuracy offered by these. Furthermore, how to make indoor navigation systems available to the public is still a great challenge. This work represents only a small part of what indoor navigation really is. As technology advances, more sophisticated and interesting solutions related to this topic will continue emerging. At the same time, more people will have access to these and they will, eventually, become part of the everyday life.

The developed application will continue to be improved and will eventually be published in the Android marketplace. Future work will focus on finding new ways to improve the application functionality regarding both the positioning algorithm and the hardware configuration. Making the system adaptable to different environments will be a top priority since the results of the distance calculations previously shown can only relate to a very specific environment.

8 ACKNOWLEDGEMENT

The authors wish to express their sincere gratitude to the Department of Electrical and Computer Engineering, Faculty of Engineering, The Open University of Sri Lanka for the support given in various phases of this project design and implementation.

REFERENCES

1 Heydon, R. (2013). Bluetooth Low Energy: The Developer's Handbook, New Jersey: Pearson.

2 Gupta, N. (2013). Inside Bluetooth Low Energy, U.S.A: Artech House.

3 Townsend, K., Cufi, C., Akiba and Davidson, R., (2014). Getting Started with Bluetooth Low Energy, Califonia: O'Reilly Media.

4 www.bluetooth.org, Bluetooth (2016). Core specification v 4.1. [online] Available at: < https://www.bluetooth.org/en- us/specification/adopted - specifications> [Accessed 3/12/2013].

5 www.bluetooth.org, Bluetooth (2016). Supplements to the Core Specification (CSS) v6. [online] Available at: < https://www.bluetooth.org/en- us/specification/ adopted - specifications> [Accessed 14/07/2015].

6 www.infoworld.com (2014). What you need to know about using Bluetooth beacons. [online] Available at:<http://www.infoworld.com/article/2608498/mobile-apps/what-you-need-to-know-about-using-bluetooth-beacons.html>[Accessed 22/07/2014].

7 www.umbel.com (2016). 15 Companies from Airports to Retail Already Using Beacon Technology. [online] Available at: < https://www.umbel.com/blog /mobile/15-companies-using-beacon-technology>. [Accessed 2016].

8 www.bluetooth.org, Bluetooth (2016). *Core System Architecture*. [online] Available at: < https://developer.bluetooth.org/TechnologyOverview/Pages /Core.aspx> [Accessed 2016].

Feasibility Study of Concentrating Solar Power Plant for Sri Lanka

E.M. Asanka Jayasundara, K.A.C. Udayakumar*

Department of Electrical & Computer Engineering, The Open University of Sri Lanka, Nawala, Nugegoda, Sri Lanka.

*Corresponding Author: email: kauda@ou.ac.lk, Tele: +942881272

Abstract – *Generating electricity from the energy of solar has minimum impact to the environment. The solar energy is a free, clean and renewable fuel which will never run out compare to fossil fuel that have been utilizing for electricity generation. The power plants which used the fossil fuel emit large quantities of carbon dioxide and other pollutants into the atmosphere. Even though in Sri Lanka, at present energy of solar is widely used to generate electricity using photovoltaic cells, due attention has not been paid to utilize the thermal energy of solar radiation to generate electricity. This paper presents the feasibility study of concentrating solar power plant in Sri Lanka. The country is closer to the equator and has the potential to generate electricity in bulk by utilizing thermal energy of solar radiation. Literature survey has been carried to identify the types of the plants available and climate condition required to have a concentrating power plant on a location. The availability of sufficient solar resources in the island and possible locations for the plant have been studied. Considering the potential locations to build CSP the best location was proposed. Plant type, capacity of the plant and required land area were also given. Finally, the cost per unit considering environmental benefit has been calculated*

Keywords: - *Concentrating solar power, Parabolic through type, Thermal storage, Technical frame conditions, Balance of plant*

Nomenclature

DNI –Direct Normal Irradiance ($W/m^{2)}$
C_p – Specific heat coefficient (J/kg. K)
T – Temperature (K)
P – Power (W)
S – Energy (J/S)
P – Density (kg/m^3 **)**
CSP – Concentrating Solar Power

1 INTRODUCTION

The use of renewable energy sources to generate electricity has been increasing significantly during last two decades. Technological advancement, cost reduction and less environmental impact are the main reasons for the use of renewable sources to generate electricity. Solar, wind, bio -mass and tidal wave become the main sources in generating

electricity. Solar photovoltaic and CSP are used to produce the electricity using solar energy. The use of solar photovoltaic is being used in many countries including Sri Lanka for generation of electrical energy.
CSP plants which utilize the thermal energy of the solar radiation to generate electricity has not been used widely till recent past. However, CSP has number of advantages such as generation of dispatchable energy, generation of electricity during the night and cloudy days. Therefore, the interest for constructing CSP plants in many countries where the sunlight is available has been growing. As a result, these plants are now being constructed in number of countries. Spain is one of the largest power producers from the CSP and number of large CSP plants are under construction in several countries including United States, India, China and North Africa.

The growth of electricity demand in Sri Lanka due to increase of population, access to the electricity and industrialization need to be met by connecting source of bulk power to the grid. This means new power plants need to be constructed to meet the future demand. At present hydro, coal, gas turbine and diesel power plants are used to generate electricity in bulk. Even though solar photovoltaic produces considerable amount of energy, still it is used to cover the power requirement of isolated consumers or used as back-up suppliers of energy. In contrary, CSP generate electricity in bulk by utilizing thermal energy of solar radiation. CSP requires large amount of direct sun light and best constructed in arid or semi-arid regions globally known as Sun Belt (Arora, 2013). Since Sri Lanka is located closer to the equator, the country does have a potential to construct CSP plant. However, introduction of a CSP to a Sri Lankan system to meet the demand has not been studied thoroughly yet. Therefore, the aim of this research work is to carry out a feasibility study to determine the capacity of a CSP in a suitable location of the country. At the end of the work the unit cost of the generation of CPS is presented. Since the CSP produces the electricity using thermal energy of the sun, the key factor to build up a CSP is the availability of solar radiation with required DIS. The climate conditions, land availability has been studied in order to meet the aim of this project. Since the CSP does not emit the pollutant to the atmosphere the unit cost has been calculated considering cost benefit due to non-emission of the pollutant to the environment.

2 REVIEW OF LITERATURE

Renewable energy sources are energy sources that do not last due to their use. Energy of solar, wind and tidal waves are fallen in to this category. Among these renewable energy sources, solar energy is the most useable source of renewable energy in the globe. The main types of solar energy systems in use today are photovoltaic and CSP. The main advantage of use of CSP technology against other renewable energy resources is that it has the capability of providing dispatchable energy using thermal energy storage system (Tamme, 2009).

It is expected that the sunniest countries should meet bulk peak and intermediate loads with the help of CSP by 2020 and base load by 2030 (Arora, 2013). It is also expected by 2050 CSP could produce 11.3 % of global electricity demand (Arora, 2013). The potential to build CSP in a country is assed based on availability of solar radiation, vulnerability of vegetation, proximity to transmission lines, availability of water bodies and flatness of the land.

Number of research work have been carried out across the globe to assess the potential of constructing CSP. It was revealed that Spain has the capacity to generate the electricity which is about 35 times higher than the electricity demand projected for the 2050. Similar research work in US done by Kirby et al. (2003), Karsteadt *et al.* (2005), Dahle *et al.* (2008). Charabi and Gastli (2010) reported that when using parabolic trough technology, a 100 MW power plant requires about 2.4 km^2 of land in Oman. In India it has been reported that about 35 – 50 MW capacity solar power plant can be set up on 1 km^2 land area. In addition to these more projects have being planned in Middle East, North African region, Australia, Latin America and South Africa (Ziuku, *et.al*., 2009)

Solar photovoltaic converts the sun's energy to electrical energy using photovoltaic cells. As the suns light hit the solar panel, the solar radiation is converted into direct current electricity. Then the direct current is converted to alternating current using the inverters. Finally, alternating current distributed to the power network. This type of solar panels is connected to the grid at the consumers' locations and the excess of electricity over the power consumption of the individual consumer is exported to the grid during day time. Even though this feeds more power to the system, large number of inverters that are connected to the grid cause power quality issues due to the harmonics.

2.1 Operating principle of concentrating solar power plant

In CSP electricity is produced using heat energy of the sun. The mirrors and lenses are used to concentrate and focus the sunlight to a thermal receiver. The thermal receiver is similar to the boiler of conventional thermal power plant. The role of receiver is to receive the sun light and convert it to heat energy. The heat is absorbed and transported to the steam generator using thermal fluid. In most of the cases the synthetic oil is used as the thermal fluid. Then the heat is converted to the electricity in the steam generator where to this heat is transported. Block schematic diagram of a CPS is shown in figure 1. After receiving the heat to the steam generator, the operating principle is similar to the conventional thermal power plant. Since the sun light is available only part of the day, the part of the thermal energy produced is stored in thermal storage tanks to produce the electricity during the time when the sunlight is not available or not sufficient. For this purpose, two tanks with hot and cold thermal fluid are available. Unlike in solar photovoltaic cells the CPS cannot use the diffuse part of the solar radiation and direct radiation is required. The land that is required to produce the required amount of power using CSP is much larger when compare with the conventional thermal power plants. This may be the negative impact to the environment due to construction of CPS.

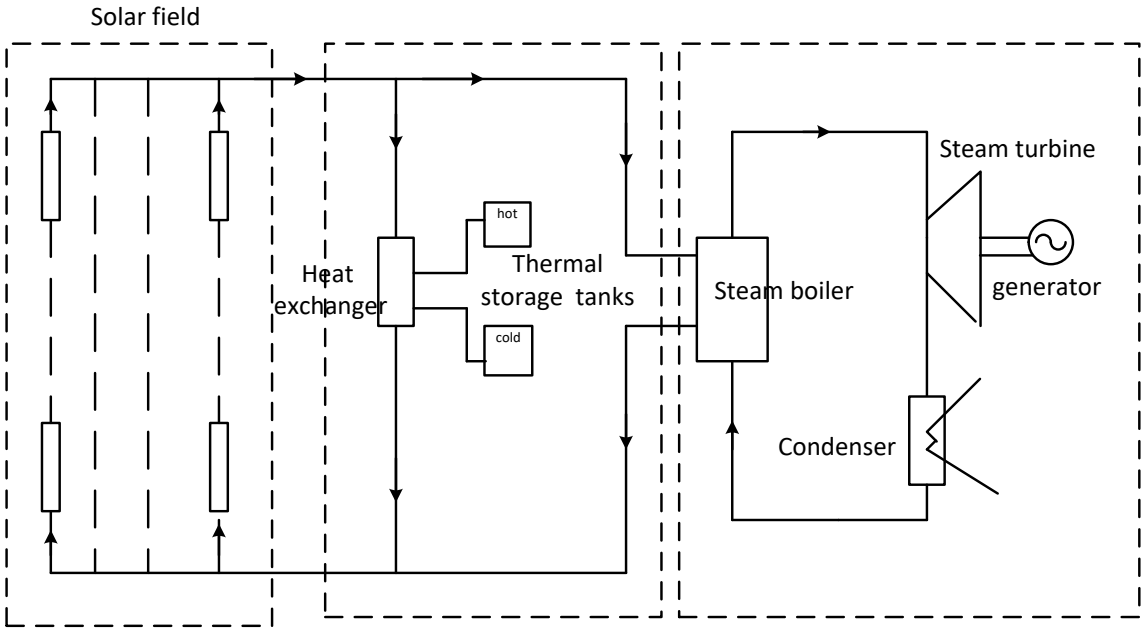

Figure 1: Diagram of a CSP plant

There are four different CSP systems: parabolic trough, power tower, parabolic dish and linear Fresnel reflector.

2.1.1 Direct normal irradiance (DNI)

The Direct Normal Irradiance is used to measure the solar energy that the concentrating solar power plant uses. This is the energy received on a surface tracked perpendicular to sun's ray. DNI provides the approximate capacity of a CSP. DNI is not a constant value and it varies throughout the day. Researches have shown that the minimum value of DNI to build concentrating solar power plant in a particular location is 2000 kWh/m^2/year (www. setis.ec.europa.eu 2014).

2.1.2 Thermal energy storage

One of the major advantages of CSP systems is their ability to dispatch power beyond the day time sun hours by incorporating thermal storage system. The storage system retains heat efficiently so that it can be stored for a day before being converted in to electricity.

Presently, thermal energy options for parabolic through and power tower systems use molten salt as the storage medium in a two-tank heat system. Two tanks thermal energy system tends to be high efficiently as energy stored is recovered at nearly the same temperature.

2.2 Suitability of concentrating solar power plant for Sri Lanka

Sri Lanka is located within the equatorial belt, and therefore the energy of sun is available throughout the year. In the South Asian region, Sri Lanka together with India, Bangladesh and Pakistan comes under countries with semi-arid areas. The countries with semi-arid regions are considered as suitable locations for constructing CSP. Within the country there are enough lands available in the dry-zone to construct these types of plants. Many of these

lands that are in dry zone are flat lands which is another requirement to have CSP. More ever, majority of these lands are not suitable for the cultivation or any other purpose and the values of them are minimum.

3 SITE SELECTION

3.1 Solar data collection

There are three sources for solar data collection: Typical Meteorological Year Data sets (TMY), surface meteorology and solar energy data sponsored by NASA and remotely collected data from meteorological department in Sri Lanka. Since the availability of sun light through the year is a key factor in designing CSP, the investigation of DNI was done for the dry zone of the country. Annual average DNI for selected locations of the country is shown in table 1. Researches have shown that the minimum value for DNI to construct CSP is 2000 kWh/m^2/year, which is equivalent to 5.45 kWh/m^2/day [Brayer and Knies 2009]. As per the data Mannar and Puthlam area are the suitable locations for constructing CSP.

.

Table 1: Annual average DNI values in different areas

Area	Annual average DNI kWh/m^2/day
Hambanthota	5.37
Mannar	5.9
Puthlam	5.88
Jaffna	5.2
Trincomaly	4.93
Anuradhapura	4.53
Vavnia	4.54
Batticalo	4.36

3.2 Factors considered in Site selection

The CSP plants require more land areas for install large number of solar mirrors. Further, the slope of the land is also one of the key factors in deciding land for CSP. The accepted landscape is up-to 3% (Brayer and Knies 2009). In this work Google earth software was used to select the number of lands that satisfies this requirement and further analyses were done to check whether other conditions also were satisfied.

Water requirement is another most important criterion since CSP needs water for steam cycle, cooling and mirror washing. However, none of the above areas (Mannar and Puttlam) does not have source of the water to be used in CSP. At the meantime, both these areas are

near to the sea and therefore desalinated water of the sea can be used for cooling purpose and mirror washing.

CSP need to be constructed in the proximity of power grid. The reason for this is to reduce the cost for transmission of energy produced by the CPS.
Access roads must be wider enough so that the large vehicles can be used for transportation of large number of parts of the solar field, heat exchangers, turbines generators etc.

3.3 Site location analysis

Considering all the factors given above Mannar area was selected as the most suitable location for constructing CSP. The area has the highest DNI value and the sufficient land is available for use. The water requirement for the plant is fulfilled by using the sea water. As the transmission lines of the grid are closer the transmission cost also can be minimized. According to the study the most suitable land is in the south-east region of the Mannar city. The site selected is 12 km away from the city (shown in figure 2) and the total area of the land is 900 x 1325 m^2 (117 ha). The cost of the land in this area is cheaper since it cannot be utilized for the agricultural purposes. Since this land is closer to the main road, the equipment of the CSP can be easily transported to the site.

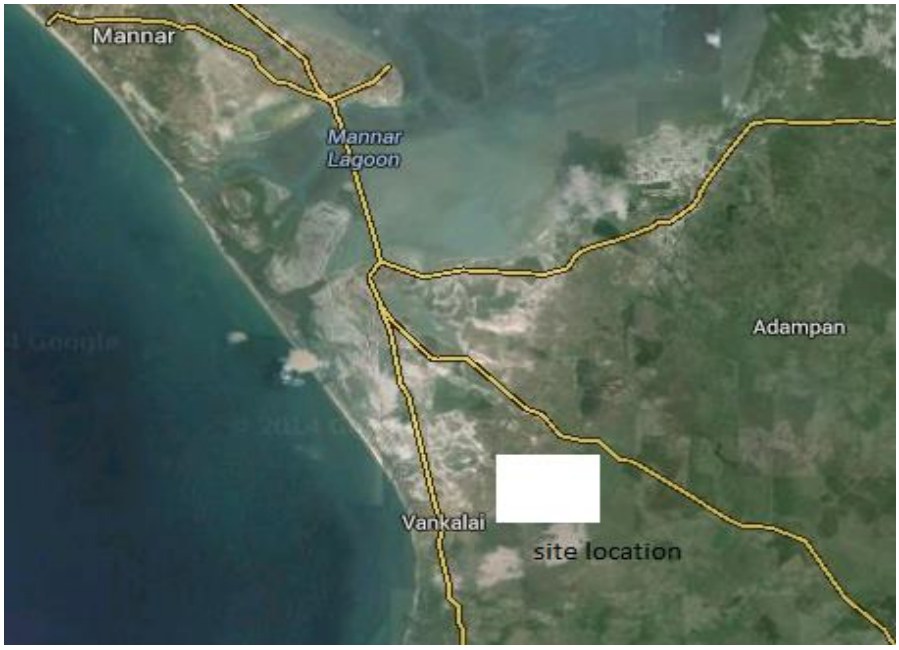

Figure 2: Site location

3.4 Average solar data in the site

The Surface Meteorology and Solar Energy Center provides monthly averaged data for last 22 years. According to the longitude and latitudes of the selected location monthly averaged DNI data was collected and shown in table 2.

Table 2: Monthly Averaged Direct Normal Radiation in the Mannar

Month	Average DNI (kWh/m²/day)
January	5.89
February	7.13
March	7.76
April	6.51
May	5.97
June	5.68
July	5.89
August	5.83
September	6.01
October	5.07
November	4.36
December	4.76
Annual average	**5.9**

4 POWER PLANT DESIGN

4.1 Modeling of solar system

Solar system modeling is the major task in CSP power plant design. Therefore, many of the solar system designers use software applications for their system modeling. The System Advisory Model (SAM) is the software which represents the cost and performance of renewable energy projects using computer models.

The selection of the solar field and suitable tracking system is important in designing CSP . In this work it is proposed to use LS-2 solar field since from the economical point of view it is one of the most suitable one for this purpose. The length and width of it are more economically suitable. .

4.2 Power plant layout

According to the land area of the site the total solar field and no of collectors which can be install in the site is calculated. Area for power block and storage also calculated.

Calculations are done according to the details of existing power plant.

Total land area = 900 m×1325m =1170000 m²

Including the power block and optimal storage the power plant land area is selected as about 4.7 times the total solar field area (Jayakumar, P. 2009).

Total area for solar field = 1170000/4.7
= 250000 m²

$$\text{No. of solar collectors for plant} = \frac{\text{total area for solar field}}{\text{collector mirror area(LS}-2)} = \frac{250000}{235} = 1064 \quad (4.1)$$

if the DNI received during 12 hours per day, the average solar insulation is calculated

$$\text{Average solar insulation} = \frac{5.9\times3600}{12\times3600} = 0.492 \text{ kW/m}^2 \quad (4.2)$$

Solar insulation in one collector = collector mirror area × average solar insulation. (4.3)
= 235 m^2 ×0.492 kW/m^2
= 115.62 kW

Considering that the collector field efficiency is 0.81 (www.nrel.gov,2015), receiver input was calculated

Receiver input = collector efficiency × solar insulation. (4.4)
= 0.81 × 115.62 kW
= 93.65 kW

Considering that the receiver efficiency is 0.88 (Arora, 2013)

Receiver output = receiver efficiency × Receiver input (4.5)
= 0.88 × 93.65 kW
= 82.41 kW

This means that thermal fluid absorbed power in one collector loop equal to the 82.41 kW.

Thermal fluid mass flow rate (m)through the receiver is given by

$$\mathbf{m = \rho AV} \quad (4.6)$$

Where

ρ = 1680kg/m^3 for molten salt
A = Receiver cross section area 0.00384m^2 (receiver diameter is 0.07m)
V = fluid velocity set to 1.2 m/s

This gives the value of m as 7.74 kg/s

If energy absorbed by heat transfer fluid is **Q**, heat transfer fluid temperature increase in one solar collector is Δt and thermal fluid specific heat $\mathbf{c_p}$ is 1520 J/kg.K the temperature increase can be calculated formula given in (4.7)

$$\mathbf{Q = m\, c_p\, \Delta t} \quad (4.7)$$

This gives the value of **Δt** as 7 K (or 7 ^{0}C)

Normally, temperature difference in hot fluid and cold is 110 ^{0}C (cold fluid temperature is 280 ^{0}C and hot fluid temperature is 390 ^{0}C). To keep this temperature difference the required number of solar collectors for one loop can be calculated.

Considering that the **Δt** is 7

No of solar collectors per loop = 110 /7 = 15.7

Required number of loops: 16

No. of solar collector loops = 1064 / 16
= 66 (4.8)

This means, 104 collectors having 66 collector loops will be installed in the area.

4.3 Plant Capacity Calculation

Using the selected site details plant capacity and storage power are calculated. All the efficiency values stated are obtained from "assessment of parabolic trough and power tower solar technology cost and performance forecasts" by Sergeant and Lundy LLC consulting group, Chicago for NREL in 2003 (www.nrel.gov ,2015).

Annual average DNI at site = 5.9 kWh/m^2/day

$$\text{Total solar field area} = \frac{\text{Tolal solar insulation}}{\text{avarage insulation}} \quad (4.9)$$

Total solar insulation = Total solar field area × average insulation (4.10)
= 250000 m^2 ×0.492 kW/m^2
= 123 MW

$$\text{collector field efficiency} = \frac{\text{Total collector output}}{\text{total solar insulation}} \quad (4.11)$$

Since the total collector output is equivalent to the total receiver input, the receiver input can be calculated

Total receiver input = collector field efficiency × total solar insulation (4.12)
= 0.81 × 123 MW
= 99.6 MW

Considering that the collector field efficiency is 0.81 (Jayakumar, 2009)

$$\text{receiver efficiency} = \frac{\text{total receiver output}}{\text{total receiver input}} \quad (4.13)$$

Considering that the Receiver efficiency is 0.88 (www.greenpeace.org, 2009) the output of the receiver can be found:

Total receiver output = receiver efficiency × total receiver input
= 0.88 × 99.6 MW
= 87.67 MW

This is the electrical power generated including the power that is stored to utilize when the sun light is not available

Next step is to calculate the amount of power that is stored. Before determining this value, it is required to calculate solar multiple. Solar multiple is the ratio of the receiver design thermal output to the power block's design thermal input. The values shall be determined by the hourly solar resource pattern.
At the site solar multiple is taken as 1.5 (according to software value 1.53).
Let the power to store is **S**.
Then,
Power to direct electricity generation = total receiver output – power to store
= 87.67 – **S**
Power to store = (solar multiple – 1) × power to direct electricity generation.
S = (1.5 -1) × (87.67-**S**)
S = 29.2 MW

Power to store is 29.2 MW
Then,
Power that goes for direct electricity generation = (87.67 -29.2) = 58.5 MW

Thermal to electrical efficiency

Net electrical power output from the plant was calculated considering the thermal efficiency of the turbine as 33%

Electrical power output = thermal to electrical efficiency × thermal power input
= 0.333 × 58.5 MW
= 19.5 MW.
Similarly, Electrical power output by storage power = 0.333 × 29.2 MW (4.14)
= 9.7MW

Plant capacity 19.5/0.9 = 21.6 MW

For 8 hours, storage energy = 9.7 MW ×8 hr
= 77.6 MWh
No of hours plant can work full load by store energy = $\frac{77.6\ \text{Mwh}}{19.5}$ = 4 hrs.

4.4 Power block

CSP requires steam turbines which are optimized for their complex and challenging cycle condition and further CSP turbine requires large number of start-up and fast daily start up capability. When focusing on annual power production, the short start up time of the turbine adds great benefits to the CSP plant.
Steam Turbine:
Considering the manufacturer data (www.siemens.com 2012), the selected turbine has following specifications:HP turbine: 100 bar , 371 °C; LP turbine: 10 bar, 371 °

Generator:

Since the output of the plant is 19.5 MW, it is proposed to install 25 MW, 11 kV generator unit for the plant. It is also proposing to install the 30 MVA, 11 kV/33 kV transformer to step up the voltage and connect to the existing 33 kV distribution line

As it was mentioned the water requirement is fulfilled by desalination of sea water. Per minute water requirement to generate 22 MW in the thermal power plant is around 66 m^3. This requires construction of desalination plant which provides demineralized water and service water. The demineralized water is for steam generator and the service water is for mirror washing and other water requirement of the plant such as firefighting systems.

4.5 Cost calculation

The cost calculation was carried out to determine the specific life cycle cost. The major cost involved in construction and operation of the plant are

(a)Direct cost	$ 82,295,000.00
(b)Indirect cost	$ 9,764,950.00
(c)Total installed cost (a+b)	$ 92,059,950.00
(d) Operation & Maintenance cost	$ 1,010,299.00
(e)Present value of O & M cost (dx9.427)	$ 9,524,095.75
Total present value of cost (c+e)	$ 101,584,045.75

The direct cost includes cost for site preparation, solar field, thermal storage power plant and cost for balance plant. The solar filed cost including cost for civil work, supporting structure, receiver, mirror and other equipment is $250 per m^2. Indirect cost includes the cost for engineering, procurement & construction and land cost.

The present value factor (Nate, 2014) was calculated considering the present worth factor (r) as 10% and plant life time (n) as 30 years:

$$\text{Present value factor} = \frac{(1+r)^n-1}{r(1+r)^n} \quad (4.15)$$

$$= \frac{(1+0.1)^{30}-1}{0.1(1+0.1)^{30}} = 9.427$$

Considering that the plant availability factor is 94% and the plant operates in full capacity during 12 hours per day, annual plant output becomes 57.85 GWh (19.5 × 12 × 263 × 0.94).

Capacity factor = 57.85 GWh /19.5 MW × 8760 h
= 33.8 %

The specific life cycle = (total present value of cost)/(present value of energy benefit)
= ($ 101,584,045.75)/545.525GWh=$0.18 /kW

Carbon credit price

When compare with the coal power plant the carbon dioxide (CO_2) emission of CPS is zero. The benefit of the CPS due non- emission of CO_2 was calculated.

In a coal power plant CO_2 emission per kWh is 0.944 kg. The total emission of CO_2 in coal power plant with similar capacity would be 54610.4 ton per annum (=0.944 kg/kWh x 57.85 GWh). This is 54610.4 carbon credits (One ton of carbon is one credit). Since the present market value of carbon is $21.25 per ton, total income from carbon credit is $ 1,160,471.00 (=54610.4 × $ 21.25)

Carbon credit price per kWh = $ 1,160,471.00/ 57.85 GWh
= $ 0.02 /kWh.

Specific life cycle cost with carbon credit cost saving = ($ 0.18 - $0.02) /kWh
= $ 0.16 /kWh
= Rs. 20.80 /kWh.

Since one Carbon credit is ton of CO_2,

Available carbon credit	= 54610.4 Ton
Present market price per tonnage	= $ 21.25
Income from carbon credits	= $ 54610.4 × $ 21.25
	= $ 1,160,471.00

(Assumption: 1 US Dollar = 130 Rupee)

5 DISCUSSION

According to the economic analysis, the specific life cycle cost of CSP was $0.18 /kWh without carbon credit earning. This value is higher than unit cost of hydro and coal but lower than high cost diesel power generation. However, inclusion of CPS as one of the energy sources to Sri Lankan power system has a prospective due to following reasons:

Cost of solar thermal technology will continue to decrease with the rapid advancement of solar technology. Therefore, in future solar thermal electricity generation cost will be competitive with conversional sources such as coal.

According to the present scenario, in future base load of the system will be covered by coal and hydro while peak load demand will have meet by the diesel power plant. Unit cost of power generation by diesel is higher than concentrating solar power.

The third is the energy mix. It is said that concentrating solar power technology is dispatchable power generation technology which can work only in higher solar radiation areas. Hence CSP is most suitable for higher solar radiation area like Mannar. Then CSP can work instead of diesel power plant like a Chunnakam.

Finally, CSP will save the emission of carbon dioxide and other hazardous gases to environment.

6 CONCLUSION

It can be finally concluded that the parabolic through type solar thermal technology is technically feasible with available solar resources in Mannar area.
It also economically feasible with specific life cycle cost of $0.16 /kWh (with carbon credit saving) than diesel power plants considering with stored peak time generation.
Further it is environmental feasible technology by saving emission of carbon dioxide and other hazardous gases generated from coal and diesel.

RFERENCES

1 Arora, P.R. (2013). A vital role of concentrating solar power plants of Rajasthan in future electricity demand of India. International Journal of Scientific and Research Publications, volume 3, Issue 6, June 2013, ISBN 2250—3153.

2 Tamme, R. (2009). Trends in CSP Technology Storage System. Solar PACES 2009. Berlin.

3 Ziuku, S., Seytini, L., Mapurisa, B., Chikodoski, D., Koen Van Kuijk. Brayer and Knies. (2009). Potential of Concentrated Solar Power (CSP) in Zimbabwe, Energy for Sustainable development.

4 www.nrel.gov (2015): Assessment of Parabolic Trough and Power Tower Solar Technology Cost and performance forecast. Sargent & Lundy, [Online]. 2, 70-139. Available at: http://www.nrel.gov/docs/fy04osti/34440.pdf [Accessed 02 /07 2014].

5 www. eosweb.larc.nasa.gov (2014). Atmospheric science Data center. 2014. Surface meteorology and Solar Energy. [ONLINE] Available at: https://www. eosweb.larc.nasa.gov/cgi-bin/sse/sse.cgi?+ss11. [Accessed 04/05 2014].

6 Dave, R. (2003). Solar Resource Assessment for Sri Lanka and Maldives. NREL, [Online]. 1, 5-20. Available at: http://www.osti.gov/bridge [Accessed 16/05/ 2014].

7 www. setis.ec.europa.eu (2014). Energy Research Knowledge Centre (ERKC), 2013. Concentrating Solar Power, [Online]. 1, 28-54.: http: //www.setis.ec.europa. eu/energyresearch/sites/default/files/docs/ERKC%20TRS%20Concentrating%2 0Solar%20Power_print.pdf [Accessed 20/01/2014].

8 www.greenpeace.org (2009). Green SPACE, 2009. Why Renewable Energy is Hot? Concentrating Solar Power Global Outlook 09, [Online]. 2, 6-70. Available at: http://www.greenpeace.org/international/Global/international/planet-2/ report/2009/5/concentrating-solar-power-2009.pdf [Accessed 10/01/2014].

9 Jayakumar, P. (2009). Resource Assessment Handbook. Solar Energy, [Online]. 2, 47 - 60. Available at: http://recap.apctt.org/Docs/SOLAR.pdf [Accessed 15/05/ 2014].

10 Kearney, A.T. (2010). Clean electricity on demand. Solar Thermal Electricity 2025, [Online]. 1, 12-32. Available at: http://www.estelasolar.eu /fileadmin /ESTELAdocs/documents/Cost_Roadmap/2010-06_-_Solar_Thermal_ Electricity _ 2025_-_ENG.pdf [Accessed 10/01/2014].

11 .Kelly, B. (2014). Parabolic Trough Solar System Piping Model. Final Report, [Online]. 1, 2-21. Available at: http://www.osti.gov/bridge [Accessed 24/05/ 2014].

12 Matthias, G., Michael, J. (2011). Parabolic Trough Technology. Advanced CSP Teaching Materials, [Online]. 5, 20-70. Available at: http://www.energy-science.org/bibliotheque/cours/1361450193Chapter%2005%20parabolic%20troug h.pdf [Accessed 10/06/2014].

13 Michael, J. (2010). A Detailed Physical Trough Model for NREL's Solar Advisor Model. NREL, [Online]. 1, 2-12. Available at: http://www.osti. gov/ bridge [Accessed 20/06/2014].

14 Nate, B. (2014). System Advisor Model, SAM 2014.1.14. General Description, [Online]. 1, 2-18. Available at: http://www.nrel.gov/docs /fy14osti /61019. pdf [Accessed 30/06/2014].

15 Renné, D., George, R., Marion, B. and Heimiller, D.(2003). Solar Resource Assessment for Sri Lanka and Maldives , [Online]. 1, 5-12. Available at: http: //www.nrel.gov/docs/fy03osti/34645.pdf[Accessed 05/02/2014].

16 www.siemens.com (2012). Steam turbines for CSP plants . [Online] Available at:http://www.siemens.com/about/sustainability/pool/de/umweltportfolio/produkte-loesungen/energieuebertragung-energieverteilung/solar-energy_steam-turbines.pdf. [Accessed 15/08/2014].

17 Siyambalapitiya, T., Perera,N.G.S., Nanthakumar, J. and Samaliarachchi,L.A. (2002). Power Systems planning. First edition. Open university of Sri Lanka.

18 www.seco.cpa.state.tx.us (2008). State energy conservation- 2008. Solar energy. [Online] Available at: http://www.seco.cpa.state.tx.us /publications / renew-energy/solarenergy.php. [Accessed 12/03/2014].

19 Stine, W. B., Michael, G. (2001). The sun's energy. Power from the sun, [Online]. 2, 1-10.Availableat: http://www.powerfromthesun. net/Book /chapter02 /chapter02.html [Accessed 07/01/2014].

Infant Cry Detection System with Automatic Soothing and Video Monitoring Functions

G.V.I.S. Silva, D.S. Wickramasinghe*

Department of Electrical & Computer Engineering, The Open University of Sri Lanka, Nawala, Nugegoda, Sri Lanka

*Corresponding Author: email: dswic@ou.ac.lk, Tele: +94718568047

Abstract - *The aim of this research is to develop a portable, efficient and cost effective automatic infant's cry detector and self-soother with real time monitoring system for employed parents.*

The cry detection algorithm has developed according to the crying signals and it is segmented using the short time energy function which is used as a voice activity detector to disable the operation of the algorithm when voice activity is not present. The features are extracted using MFCC (Mel Frequency Cepstrum Coefficients) and pitch frequency. Statistical properties are calculated for the extracted features of MFCC and pitch frequency. K-NN (K-Nearest Neighbour) algorithm classifier is used to classify the cry signal. The system can easily identify the infant cry and it is verified using K-NN with accurate results by proposed detection algorithm.

The combination of Pitch and MFCC gives more promising approach to cry detection than using only MFCC. The total average accuracy of MATLAB simulation is 80.8335% and on the device accuracy was77.5% for cry detection.

Immediate cry detection and self-soothing system helps to increase baby's cognitive development process. This all in one module approach gives great benefits to the first-time parents, adoptive parents, caretakers, researchers or physicians by both economically and scientifically.

Key words – ***Cry detection, MFC, K-NN, Pitch detection, Soothing system***

1 INTRODUCTION

Infant cry is the first verbal communication of new born baby with the world. The crying of the infant is a common phenomenon and probably one of the most difficult problems which parents have to face when taking care of a baby.

The cry of an infant is a biological siren to alert for the care giving environment about their needs to motivate the listener to respond. Most of the times, caretaker's advocates' follow strict routines to train the child for regular feeding, waking and sleeping pattern without considering their emotional and physical needs. Researchers have found babies whose cries are usually ignored will not develop healthy intellectual and social skills [15].On the other hand, leaving a distressed baby to cry on a regular basis could damage the brain development.

Currently there are many types of baby monitoring systems with wearable option, android applications, wirelessly controlled camera systems etc. Most of these systems are

covered only home using Wi-Fi or Bluetooth. Due to this condition, employed parents (especially mothers) cannot ensure the safety of their babies because, they are unable to connect with the child when they're at working places. There are few products which have remote monitoring facilities. However, those are priced high-end products which are not affordable in developing countries like Sri Lanka. Further, these products are not easy to set up and by fixing near to the baby may cause health hazards due to electromagnetic radiation.

This product is designed for an affordable cost and it can be used from birth to 12 months of babies with ability to detect the infant's crying immediately and send notification to warn parents/caregiver while a soft sound and lights playing to sooth the baby. On the other hand, if the parent has any doubt about babies, they can connect to the home wireless network and check the baby using a mobile phone in real time at any time while ensuring the safety of the baby. The other benefit of this product is, it is important for hearing impaired parents because the parent can get notifications through android application which is password protected, and hearing-impaired parent can configure their phone into the vibration mode. Parents can watch live video stream from the baby's room when the notification received.

2 OBJECTIVES

This research work was carried out to achieve the following objectives,

(a) Study feature extraction methods in audio processing and develop a cry detection algorithm in different approaches of feature extraction and classification methods.

(b) Design and implement infant's cry detection device, by applying the developed cry detection algorithm with self-soothing and video monitoring functions.

3 LITERATURE REVIEW

3.1 Theoretical Background

Automatic Speech Recognition systems (ASR)

Automatic Speech Recognition (ASR) is the process of converting a speech signal to a sequence of words, by means of an algorithm. Five modules can be identified to develop an ASR. [1]

i. Speech Signal acquisition.
ii. Feature Extraction.
iii. Acoustic Modelling.
iv. Language & Lexical Modelling.
v. Recognition.

Feature extraction requires more attention in speech recognition because recognition performance depends heavily on this phase. The main goal of the feature extraction step is to compute a parsimonious sequence of feature vectors providing a compact

representation of the given input signal. The feature extraction is usually performed in three stages. The first stage is called the speech analysis or the acoustic front end. It performs Spectro temporal analysis of the signal and generates raw features describing the envelope of the power spectrum of short speech intervals. The second stage compiles an extended feature vector composed of static and dynamic features. Finally, the last stage transforms these extended feature vectors into more compact and robust vectors that are then supplied to the recognizer. [1]

There are various techniques used for feature extraction. Cepstral Analysis, Mel Cepstrum Analysis, Mel-Frequency Cepstrum Coefficients (MFCC), Linear Discriminant Analysis (LDA), Fusion MFCC, Linear Predictive Coding (LPC) Analysis and Perceptually Based Linear Predictive Analysis (PLP) are some of the techniques being used.

After feature extraction, the most important step is speech recognition. Basically, there are three approaches of speech recognition [1]. Those are Acoustic Phonetic Approach, Pattern Recognition Approach and Artificial Intelligence Approach.

3.2 Literature survey of similar products

Comparison of similar products is shown in table 1.

Table 1: Comparison of similar products in the market for baby care with cry detection

Product name	Methodology	Price	Drawbacks
Why Cry – Baby Cry Analyzer Monitor [7] 	This sound sensitive device is programmed to recognize different pitches and then digitally analyses and transmit the baby's cry into one of five simple expressions – hungry, bored, annoyed, sleepy or stressed.	US$ 52.34 (LKR ~7800)	1. No real time video monitoring option 2. No self-soothing system included 3. The alarm is sound based, need to be in the range to hear the alarm
Wireless Baby Crying Detector with Parental Alarm[8] 	This crying detector consisting with transmitter and receiver. Once the baby cry or other noise occurs, the receiver starts to make electronic crying noise. It's a low cost and compact design.	US$ 10.70 (LKR ~1600)	1. Low sensitivity of cry detection 2. Alarm is sound based and not useful for hearing impaired 3. No self-soothing system included 4. Limited Range (in between 50-60 m)

Cry translator 	A simple and lightweight. It is designed to be handled with one hand and attend to baby with the other. Notify the reason for crying. Can soothe baby with the sound of the beating of a heart or lullabies.	79.90 € (Euro) (LKR ~12800)	1. No alarming system to care giver when baby needs attention 2. Expensive 3. Limited range /No real time video monitoring option.
Wi-Fi, baby 2.0 	This monitors video and hear audio from the baby's room via an iPad, iPhone, PC, Mac, Android phone, or Android tablet. The video and audio streams live from a single Wi-Fi Baby unit set up in the child's bedroom.	**US$ 230** (LKR ~34500)	1. Do not detect the crying of a baby 2. Always need to watch the baby video and pay attention to the audio. 3. Only covers home wireless network

4 METHODOLOGY

The block diagram of the proposed system is shown in Figure 1. This system consists of 2 units; child unit and parental unit.

The child unit consists with a data processing unit, which interfaces with camera, speaker, microphone and self-soothing system with wireless connectivity (Wi-Fi). For the data processing, single board computer has been used. Parental unit is a smart phone, laptop or tablet with internet connectivity. Child unit connected with home internet connections via Wi-Fi or Ethernet. Parental unit and child unit are connected via internet. A notification will be given to the parent if baby is crying continuously. Then the parent can operate the system remotely according to his or her wish. It can be connected to the internet and can check his/her child online with a mobile phone in real time.

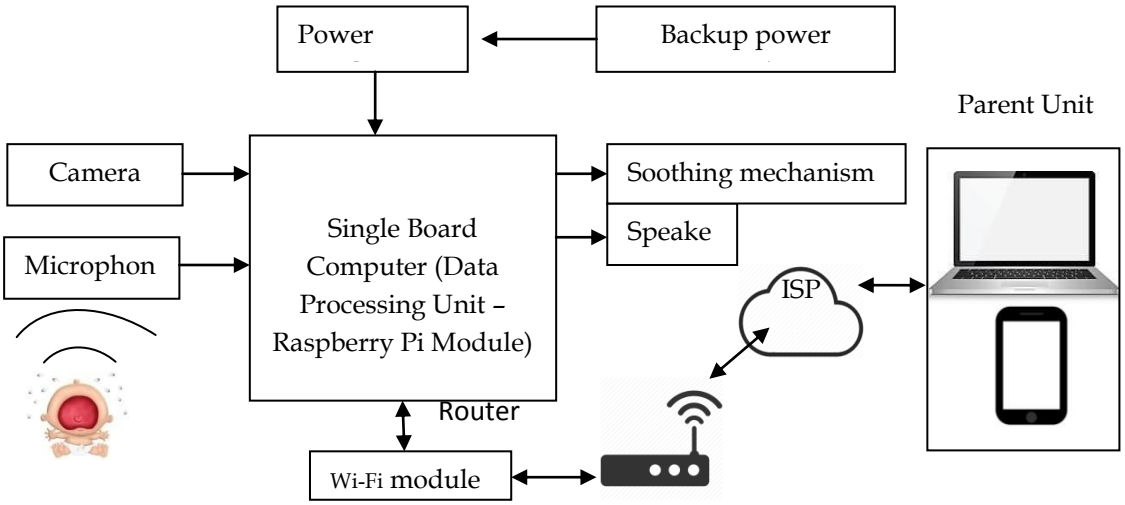

Figure 1: Block Diagram of the proposed infant cry detection and soothing system

Automatic cry detection system

When the baby starts crying, at a predetermined time a microphone picks up a cry from the baby as an audio signal. At a certain sampling frequency, an A/D converter samples the audio signal received by the microphone and convert it. An audio Analyzer analyze the audio signal samples by the A/D converter and computes a characteristic quantity based on a frequency spectrum (Feature extraction).
After signal processing, data processing unit classifies the pattern from a recognition model by training it with infant cry samples (reference) and give the decision logic whether it is crying or not.

Self-Soothing system

When the cry detection algorithm detects the sound input as cry at a predetermined time, a signal given to the two DC motors and 1st rotating lamp will be rotated continuously while the 2nd rotating lamp gives glow effect. Furthermore, the glowing effect can use the black perspective sheets with beautiful carvings which includes base to project different shapes on ceilings or walls, also according to different colours, these sheets can be changed manually, which will be very user friendly, and gives more realistic output to the baby at his developmental stage other than being bored by seeing the same light effect. The projection shapes and colours have been selected according to research papers [14] which are based on cognitive development of child at infancy period. In raspberry PI module (Single Board Computer), easily can operate the self-soother by using GPIO (General Purpose Input Output).

LED illusion mirror effect can be used for more glow effect and it affect to the babies' visual systems development, and at just 3 months of age, they have appeared perceive colours in a way that is analogous to adults. And simultaneously with the above process plays his favorite lullabies, or white noises soothe him, which are stored in raspberry PI as a sound library, after this sequence if baby continuously crying then notification will be sent to the parent.

From the proposed product, parents get instant notification when a cry detected. They can control (Playing music, call on their own voice) the soothing mechanism. Also, from live video streaming feature, parents can view their child real time. Further, crying sample can be saved for later statistical analysis.

The design of the system consists with two main subsystems.

- Cry detection algorithm
- Soothing mechanism and video streaming function

Overall integration of various modules also part of the design. Figure 2 shows the flow chart of the overall system.

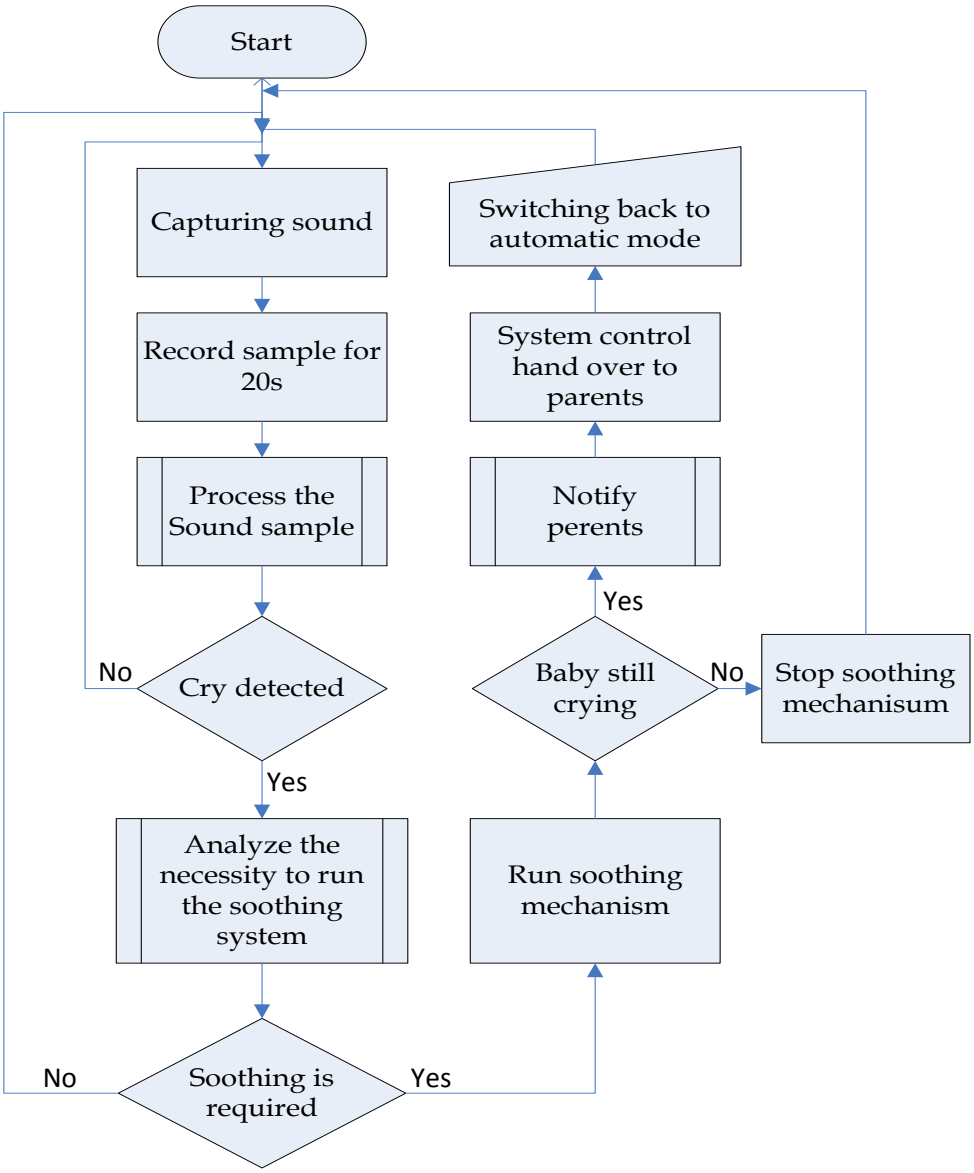

Figure 2: Top level flow chart of the system

4.1 The Cry Detection Algorithm

The proposed algorithm is composed of three main stages:

i) ***Voice Activity Detector (VAD)*** for detecting sections with sufficient audio activity. Short time energy is used as a VAD.

Short-time energy:

Where $E_n$is the energy of the sample 'n' of the audio signal, x [m] is the discrete time signal and w[m] is a rectangle window of size 'N'. The rectangle window function is defined by the expression below: w[n] = 1, 0 ≤n≤N-1; else w[n] =0

$$E_n = \frac{1}{2N}\sum (x[m].w[n-m].w[n+m])^2$$

ii) ***Feature to be extracted***

As mentioned in the section 3.1, there are various methods to extract the feature of the audio signal. In the proposed algorithm, two features have extracted from the cry audio signal.

Pitch: It's a fundamental frequency of a periodic wave form. In humans, pitch is determined by the frequency of the vibration of vocal chords.

- Adult males average at 120 Hz, [85,155]
- Adult females average at 210Hz, [165, 255]
- Infants average at 450hz, [250, 700]

Modified autocorrelation Method used for detecting the fundamental frequency of the infant cry based on the center clipping method which gives more accurate results.

Steps of Modified Auto Correlation Method for Pitch Frequency extraction [6]

Figure 3 shows the block diagram of the pitch detection algorithm. The segmented audio signal is first required to be low pass filtered to 900Hz. Then the signal is digitized at a 10 kHz sampling rate and sectioned into overlapping 30ms (300 samples) sections for processing. Since the pitch period computation for all pitch detectors are performed 100 times/s, every 10ms, adjacent sections are overlapped by 20ms or 200 samples. The first stage of processing is the computation of a clipping threshold *CL* for the current 30-ms section of speech. The clipping level is set at a value which is 68% of the smaller of the peak absolute sample values in the first and last 10-ms portions of the section. Following the determination of the clipping level, the 30-ms section of the speech is center clipped, and then infinite peak clipped. Thereafter, clipping the autocorrelation function for the 30-ms section is computed over a range of lags from 20 samples to 160 samples (2-ms-20-ms period). Additionally, the autocorrelation at 0 delays is computed for voice/unvoiced determination. The autocorrelation function is then searched for its maximum value. If the maximum exceeds 0.55 of the autocorrelation values at 0 delays, the section is classified as voiced and the location of the maximum is the pitch period. Otherwise, the section is classified as unvoiced.

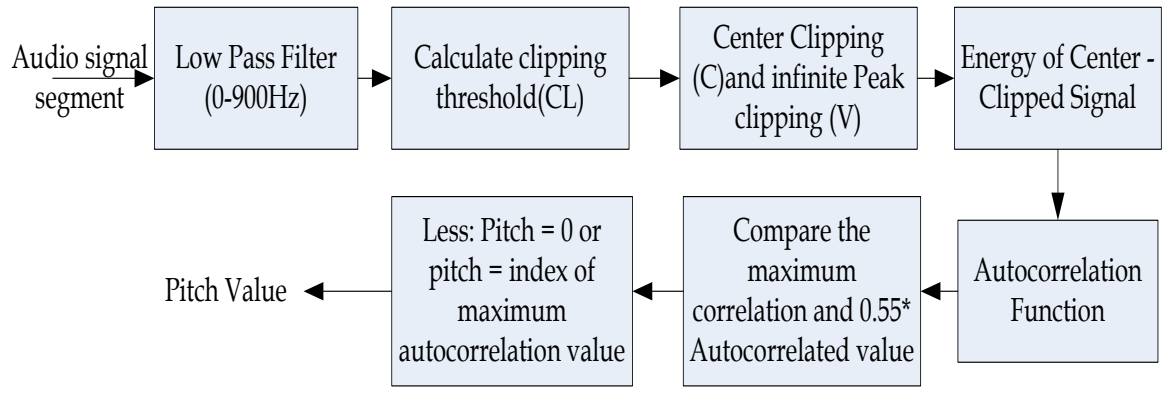

Figure 3: Block diagram of pitch detection algorithm using the modified autocorrelation method

Mel-Frequency Cepstrum Coefficients (MFCC)

MFCC provides a representation of the short-term power spectrum of a signal. These coefficients are obtained by multiplying the short-time Fourier Transform (STFT) of each analysis frame by a series of *M* triangularly-shaped ideal band-pass filters, with their central frequencies and widths arranged according to a Mel -frequency scale. The total spectral energy *E*[*i*] contained in each filter is computed and a Discrete Cosine Transform (DCT) is performed to obtain the MFCC sequence.

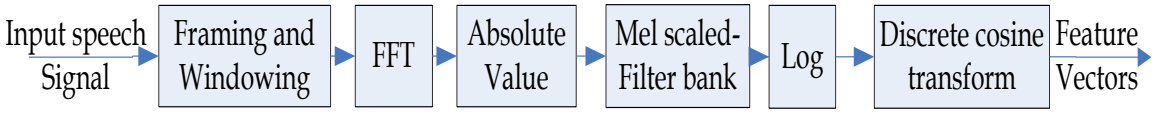

Figure 3: Steps to calculate MFC coefficients

Framing and Windowing: -First split the signal up into several frames such that, analysing each frame in the short time instead of analysing the entire signal at once. At the range (10-30) ms, most part of speech signal is stationary. It is necessary to work with short term or frames of the signal. Windowing is performed to avoid unnatural discontinuities in the crying segment and distortion in the underlying spectrum. The choice of the windowing is a tradeoff between several factors. In speaker recognition, the most commonly used window shape is the hamming window [3].The hamming window W_H (n), defined as,[6]

$$W_H(n) = 0.54 - 0.46\ cos\left(\frac{2n\pi}{N-1}\right)$$

The hamming windows is used since, MFCC will be used which involves in the frequency domain. (Hamming windows will decrease the possibility of high frequency components in each frame due to such abrupt slicing of the signal.)

Fast Fourier Transform (FFT): To convert the signal from time domain to frequency domain preparing for the next stage (Mel frequency wrapping).Spectral analysis shows that cry signals have different timbres in speech signals correspond to the different energy distribution over frequencies. Therefore, usually perform FFT to obtain the magnitude, frequency response of each frame.

Mel-scaled the filter bank: The speech signal consists of tones with different frequencies. For each tone with an actual Frequency, f, measured in Hz, a subjective pitch is measured on the 'Mel' scale. The *Mel-frequency* scale is linear frequency spacing below 1000Hz and a logarithmic spacing above 1000Hz.Using the following formula to compute the Mel(f) for a given frequency *f* in Hz:

$$\text{Mel(f)} = 2595 * \log_{10}(1 + \text{f}/700)$$

One approach to simulate the subjective spectrum is to use a filter bank; one filter for each desired Mel frequency component. The filter bank has a triangular band pass frequency response, and the spacing as well as the bandwidth is determined by a constant Mel-frequency interval.

The reasons for using triangular band pass filters are twofold:

- Smooth the magnitude spectrum such that the harmonics are flattened to obtain the envelope of the spectrum with harmonics.
- Reduce the size of the features involved.

Discrete cosine transforms, or DCT: In this step, we apply DCT on the 20log energy E_k obtained from the triangular band pass filters to have L Mel-scale Cepstral coefficients. The formula for DCT is shown below.

$$C_m = \sum_{k=1}^{N} \text{Cos}\left[\frac{m(k-0.5)\pi}{N}\right] E_k \, , m = 1,2, \ldots \ldots L$$

Where N is the number of triangular band pass filters, L is the number of Mel-scale Cepstral coefficients. Usually we set N=20 and L=12. Since we have performed FFT, DCT transforms the frequency domain into a time-like domain called quefrency domain. The obtained features are similar tocepstrum; thus, it is referred to as the Mel-scale Cepstral coefficients, or MFCC.

iii) Classification using k-nearest neighbours (k-NN) algorithm

This algorithm operation is there to compare a given new record with training records and finding training records that are similar to it. It searches the space for the k training records that are nearest to the new record as the new record neighbours. In this algorithm nearest is defined in terms of a distance metric such as Euclidean distance. Euclidean distance between the two records (or two points in n-dimensional space) are defined by:

If $x_1 = (x_{11}, x_{12} \ldots x_{1n})$ and $x_2 = (x_{21}, x_{22} \ldots x_{2n})$

$$\text{dist}(X_1, X_2) = \sqrt{\sum_{i=1}^{n} (X_{1i} - X_{2i})^2}$$

Where x_1 and $x_2$are two records with n attributes. This Formula measures the distance between two patternsx_1 and x_2.The K-nearest neighbour classifier is a supervised learning algorithm where the result of a new instance query is classified based on the majority of the k-nearest neighbour category.

4.1.1 Methodology of Infant Cry Detection

The aim of the detection algorithm is to classify each incoming segment of a stream of input audio signals as 'cry' or 'no cry' The algorithm analyses the signal at various time-scales (segments of several seconds, sections of about 1 second, and frames of several tens of milliseconds). Figure 4 shows the audio processing algorithm to detect cry signal.

- A VAD is applied and the amount of activity is calculated for each segment.
- Each segment is further divided into sections of 1 second, with an overlap of 50%.
- If the activity duration of a given section is below toa predefined threshold (30%) [4], the section is considered as having insufficient activity, and is classified as 'no cry' or '0'.

- If the activity is above the threshold, the section is divided into short-time frames (with duration of 32 msec and a hop size of 16 msec). [4]
- Each frame is classified either as 'cry' or as 'no cry', based on its extracted features using a k-NN classifier.
- For each section, if at least half of the frames are classified as 'cry', the whole section is considered as 'cry', Otherwise, it is considered as 'no cry'.
- Use K-NN classifier to classify the data *in* which each frame is classified either as a crying sound ('1'), if close enough to cry training samples, or as 'no cry' ('0'). The signal is divided into consecutive and overlapping segments, each of 10 seconds, with a step of 1 second.

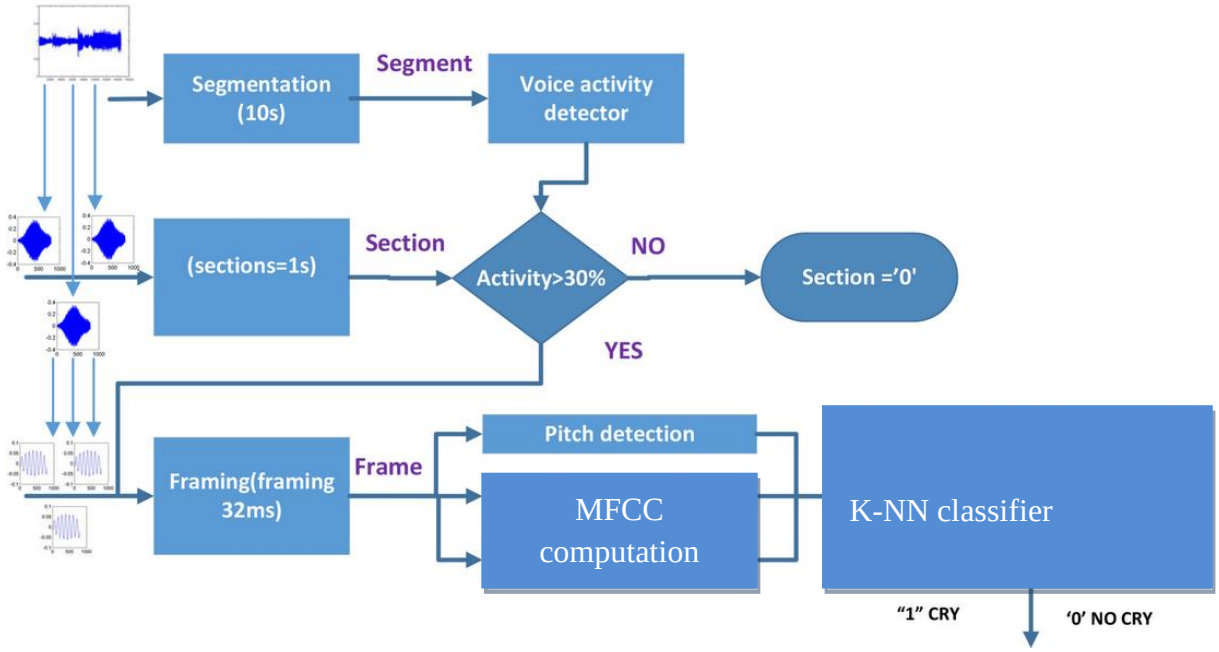

Figure 4: Infant cry detection algorithm –block scheme

5 IMPLEMENTATION

Implementation has done in three steps.

1) Hardware implementation
2) Implementation of audio processing
3) Implementation of video streaming, parent monitoring and notification system

5.1 Hardware Implementation

For the prototype, Raspberry A+ Single board computer has been used. Main reasons for the selection is, its support multimedia and it has enough processing power and memory capacity to process audio processing algorithms introduced in section 4.

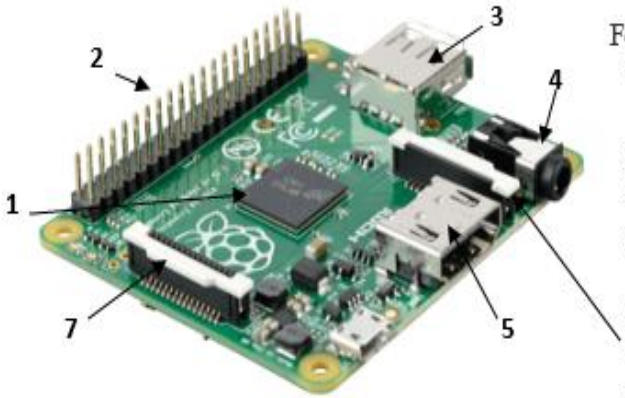

Features

1	700MHz Broadcom BCM2835 CPU 256MB RAM
2	40pin extended GPIO
3	1 x USB 2 port
4	4 pole Stereo output and Composite video port
5	Full size HDMI
6	CSI camera port
7	DSI display port

Figure 5: Raspberry Pi A+ single board computer and its components

For the video calling feature, Raspberry Pi compatible 5Mega pixel camera module has been used. This module capable of 1080p video and still image and it can connect to Raspberry Pi directly with CSI (Camera Serial Interface).Speaker system integrated via Raspberry Pi via USB hub. It has built in microphone and able to pay and store music files in MP3 format.

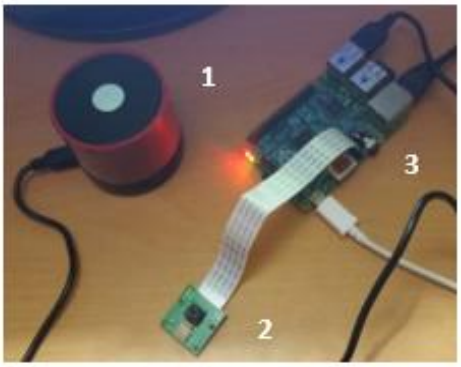

Components

1	USB compatible Speaker system
2	Raspberry compatible 5MP camera
3	Raspberry Pi B+ board (for testing purpose)

Figure 6: Interconnection of Speaker, Camera and Raspberry PI board.

Implementation of the Soothing system

Figure 7: Implementation of Soothing system (Mechanical and Electronic circuit)

Figure 7 shows the implementation of the mechanical arrangement of the soothing system. The right-hand side picture shows the fabrication of the Microcontroller based soothing control system.

5.2 Implementation of Audio Processing Algorithms

All the audio processing algorithms first implemented and tested in MATLAB 2014b environment. Later MATLAB Code converted to C code and uploaded to the Raspberry Pi board. In order to test the system, various crying samples are required.

Data collection
The large number of baby cries has been recorded from daycare centers, neighbours and online databases, then fed to the computer. The signal is stored on the computer as a lossless WAV PCM file. Cry signals of babies ranging in age between 0-15 months. Collected data mainly has 3 voice domains; voice of baby, voice of the adult and mixture of baby & adult. It is assumed all the babies were healthy, Noise free environment (not engaged with engines, passersby, car horns, high hammering sounds, etc). Downloaded baby laugh/ splashes/ sneezing/ music and rattle sounds /giggles /happy vocals ranging between 0-15 months as negative samples. There are 150 training data, each of which represents the all sound forms, including cry and non-cry. 120 testing data are there respectively, including cry and non-cry.

Testing the Algorithm in MATLAB

According to the algorithm,

- **Sample Data-**Sample data is the data that use instantly to check the results, according to the accuracy of the system simulations, we can change the sample size which we input to the system. The example MATLAB code is shown in Figure8.

- **Training Set-**It is the set that installed in the programmed memory and it used for distance calculation with sample data, 45 data set as the training set. With 37 babies cry samples and 08 non-cry samples and after that, gradually increased the training set 45 to 75 and 75 to 120 samples and 120 to 150. MATLAB implementation is shown in Figure 9.

- **Group Matrix-**This matrix defines the domains (baby cry domain, baby non-cry domain) of each and every data in training set.

- **Output -**Output is given according to the input sample size, each sample input data is calculated with each and every data in training set. All data in the training set are defined in the Group matrix as it belongs to cry or not. As an example, consider a one sample data, this sample is calculated with each and every data in the training set for obtaining the distance values and find out shortest distance given by which training data, then according to definition of group matrix algorithm identify the nearest neighbours of the sample data. MATLAB output results shown in Figure 10.

```
Command Window
>> % Matlab Function - knnclassify
% Syntax :
% Class = knnclasify(sample,training,group)

%Sample Matrix
A = [
    0.704,558.2278;
0.683,525.2134;
0.895,760.3448;
0.702,490;
0.955,958.6957;
0.937,938.2979;
```

Figure 8: MATLAB code of Training matrix

```
%Training Matrix
B = [
0.688,450.7042;
0.595,324.2647;
0.625,412.1495;
0.655,428.1495;
0.750,588;
0.712,472.596;
0.698,490;
0.795,572.7273;
0.760,604.1096;
0.757,595.9459;
0.775,612.5;
0.785,630;
0.735,537.8049;
0.699,501.136;
0.715,495.5056;
0.698,479.3475;
0.778,621.1268;
0.812,711.2903;
0.789,630;
```

Figure 9: MATLAB code of sample matrix

Figure 11 shows the MATLAB plot of variation Pitch Frequency against MFCC values. It confirms the other research finding, infant pitch frequency between 350-700Hz.

```
%Function
Class = knnclassify(A,B,G);

% Display result
disp('Result:');
disp(Class);
Warning: KNNCLASSIFY will be remo
data using ClassificationKNN.pred
> In knnclassify at 80
Result:
     'CRY'
     'CRY'
     'CRY'
     'CRY'
     'NOTCRY'
     'NOTCRY'
```

Figure 10: Output of KNN algorithm

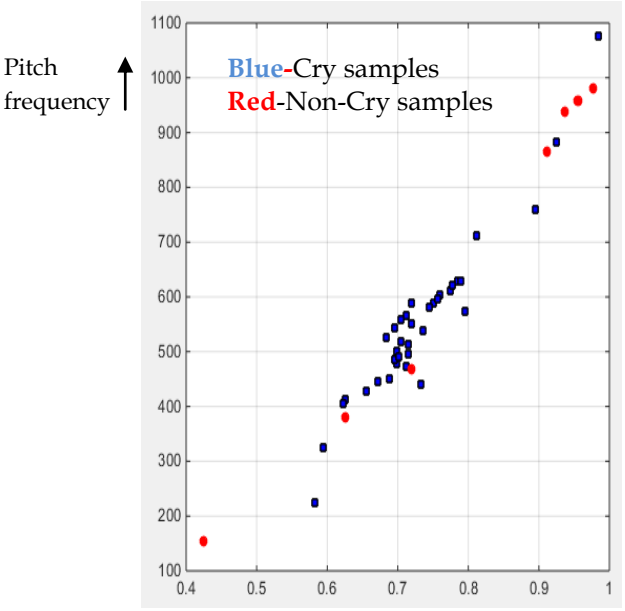

Figure 11: Graph of MFCCv'ss Pitch Frequency

5.3 Implementation of parent device application and video calling function

Parent device of the infant cry detection system is an android application which can be installed on a smart phone or a tablet computer. Once it linked to the home wireless network, users can install the application on the mobile device and have unlimited access to the video feed from the baby's room. The application is password protected to prevent outsiders from gaining access (Figure 12).

The login screen gives the IP address to connect the device after typing correct user name and pass word it enables to connect to the system. Then the application gives the option to on/off the self-soothing notification on the user's mobile device. By clicking on the top of the right side of the application (three dots) will give the user to disconnect or turn off the device.

Video calling feature implemented using available application called "VLC player". It has been installed and configured with the Raspberry Pi Operating system.

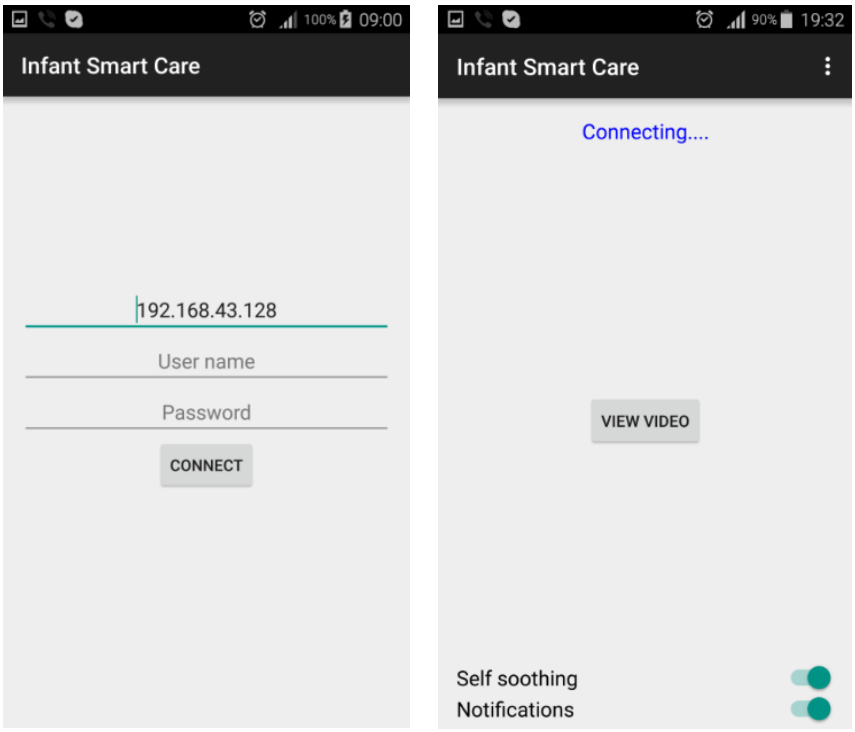

Figure 12: Menus of the Android application

6 RESULTS AND DISCUSSION

In this testing phase 150 training sample, and testing samples with 6 types of cry samples which have each 10 samples, as positive testing samples, and 60 testing negative samples to evaluate the performance of the algorithms. Testing was carried out in both MATLAB simulation and Raspberry Pi based prototype device.

When downloading and recording cry/laugh samples have been categorized mainly as above mentioned 12 categories, in this simulation it's detected only whether its cry or not cry. Table 2 shows the summary of testing results.

MATLAB simulation shows the cry detection accuracy 81.667% and on device shows the 78.33% accuracy which means low accuracy output than the MATLAB simulation results, this is because the MATLAB is a total theoretical simulation, but when testing it in practically there are some other noises can be added to the system, 60 negative samples shows 80% of non-cry detection accuracy and the device shows 76.667% non-cry detection accuracy. This means the average classification accuracy of the device is 77.5%.

Table 2: Summary of Test results in MATLAB Simulation and on Device

Positive	**Test Samples**	**MATLAB simulation**		**Accuracy**	**On device**		**Accuracy**
		Detected as cry	**Detected as non-cry**		**Detected as cry**	**Detected as non-cry**	
Pain	10	9	1	90%	9	1	90%
Screaming	10	8	2	80%	8	2	80%
Yell moan	10	9	1	90%	8	2	80%
frustrated	10	8	2	80%	7	3	70%
Whining	10	8	2	80%	7	3	70%
Upset	10	7	3	70%	8	2	80%
				81.667%			78.333%
Negative	**Test samples**	**MATLAB simulation**		**Accuracy**	**On device**		**Accuracy**
		Detected as non-cry	**Detected as cry**		**Detected as non-cry**	**Detected as cry**	
laugh	10	8	2	80%	8	2	80%
Happy vocal	10	7	3	70%	7	3	70%
giggles	10	8	2	80%	8	2	80%
gurgle	10	9	1	90%	8	2	80%
Adult baby speech mixture	10	7	3	70%	7	3	70%
Music play/rattle sounds	10	9	1	90%	8	2	80%
				80%			76.667%

Table 3 shows how is the effect of increasing number of training samples can increase the accuracy of the system.

Table 3: Effect of the increasing of Number of samples

No of training samples	MATLAB simulation	On Device
45	65.75%	60.22%
75	72.356%	68.003%
120	77.22%	73.58%
150	80.8335%	77.5%

Proposed infant cry detection algorithm is based on 2 decision levels in different time scales and classified either as 'cry' or 'non-cry' based on its spectral characteristics.

Multiple time scale analysis and detection levels are aimed in providing a classifier with high detection rate, whether the total average accuracy up to now is 80.8335% (Simulation) and 77.5% (On device).This can be improved by adding more training data

to the system as reference to the sample matrix. The detection rates fall in relatively broad range, whereas missed detection rate has a narrow range.

The main objective of this study is the development of a cry detection algorithm by applying different approaches in feature extraction and classification. Results show the developed algorithm working with acceptable accuracy. However, Soothing system needs to be tested with the real environment to test how babies responded to the soothing mechanism which is not done under this study. Also, feedback from parents about the overall product should take into consideration, before moving to the next level.

7 CONCLUSION AND FUTURE WORK

With the help of the proposed cry detection algorithm, it can easily identify the infant's cry and verified it by using KNN with accurate results. Other than using only MFCC, the combination of Pitch and MFCC gives a more promising approach to cry detection.

Employed statistical model based voice activity detector in order to determine when is the cry detection algorithm should analyse the input signal. This leads to reduction of power consumption. All of these can improve the recognition accuracy.

Cry detection has been challenging because of the highly variable nature of input speech signals. Speech signals in training and testing sessions can be different due to many facts such as:

- Baby's voice change with time
- Health conditions. For example-deaf/asthma
- Speaking rates
- Variations in recording environments play a major role.

Therefore, increasing more training samples of different noises and speeches would give more accurate results.

Future work:

- Improve the Accuracy of the cry detection algorithm by training with more samples.
- Test the soothing system in real environment and get parents' feedback regarding the overall product.
- Improve the audio processing algorithm to detect and notify the reason for baby cry.
- Improve the android application with more features.

REFERENCES

1. Therese S. S. and Lingam, C. (2013). Review of Feature Extraction Techniques in Automatic Speech Recognition International Journal of Scientific Engineering and Technology [Online] Volume No.2, Issue No.6, June pp : 479-484 Available from: http://ijset. com/ijset/ publication/v2s6 /paper 606.pdf [Accessed:24/02/2015]

2. Desai, N., Dhameliya, K. and Desai, V. (2013). Feature Extraction and Classification Techniques for Speech Recognition International Journal of Emerging Technology and Advanced Engineering[Online] Volume 3, Issue 12, December pp:367-371 Available from: http:// www.ijetae. com/files/ Volume3Issue12/IJETAE_1213_64.pdf[accessed:24/02/2015]

3. Dhingra, S.D., Nijhawan,G. and Pandit, P. (2013). Isolated Speech Recognition Using MFCC And DTW [Online] Vol. 2, Issue 8, August Available from: http: //Www.Ijareeie.Com/ Upload/ 2013/ August/ 20P_ ISOLATED. Pdf [Accessed:24/07/2015]

4. Cohen, R. and Lavner,Y. (2012). Infant Cry Analysis and Detection IEEE 27-th Convention of Electrical and Electronics Engineers in Israel [Online] November Available from: http://spl. telhai.ac.il/ speech/splnews/ upload /Baby%20 cry%20 analysis.pdf[Accessed:24/02/2015]

5. La Gasse, L. L., Neal, A. R. and Lester, B. M. (2005). Assessment Of Infant Cry: Acoustic Cry Analysis And Parental Perception Mental Retardation And Developmental Disabilities Research Reviews [Online] Volume11, December pp: *83–9* Available from:http://homepage .psy.utexa. . Edu/ homepage / group /Neallab/pubs/assessment_cry.pdf[Accessed:24/02/2015]

6. Tan, L. and Karnjanadecha, M. (2003). Pitch Detection Algorithm: Autocorrelation Method and AMDF [online] Available from http:// five dots. coe.psu.ac.th/~montri/Research/Publications/iscit2003_pda.pdf[accessed:28/07 /2015]

7. www.amazon.com (2015). Why Cry Mini Baby Cry Analyzer / Sleepy+ Stressed +Hungry[Online]Available from: http://www.amazon.com/WhyCry-Analyzer-Sleepy-Stressed Annoyed/d p/B00IALBAD2 [Accessed:24/02/2015]

8. www.dx.com(2015). Wireless Baby Crying Detector with Parental Alarm [Online] Available from:http://www.dx.com/p/wireless-baby-crying-detector-with-parental-alarm 13394?utm_source= dx&utm_medium=club&utm campaign =club_skureview_page#.VPDvznyUeyI[Accessed:24/02/2015]

9. www.amazon.com (2015). Raspberry-Pi-Model-A [Online] Available from: http://www.amazon.com/Raspberry-Pi-Model-A 256MB/dp/B 00PEX 5TO/ref=sr_ 1_fkmr1_1?s=electronics &ie=UTF8&qid=142585 76&sr=1-1-fkmr1& key words =raspi+a%2B[Accessed: 24/02/2015]

10. www.cpsc.gov/en/ (2015). FAQs: Safety Standard for Children's Toys [online] Available from: http:// www.cpsc.gov/ Business--Manufacturing/Business-Education/Toy-Safety/[Accessed: 24/02/2015]

11. *Ian Poole* www.radio-electronics.com (2015). IEEE 802.11n Standard [Online] Available from:http://www.radio-electronics.com/info/wireless/wi-fi/ieee-802-11n.php [Accessed: 24/02/2015]

12. wikipedia.org (2015). Sudden infant death syndrome [Online] Available from: http://en.wikipedia.org/wiki/ Sudden _infant_death_syndrome [Accessed: 24/02/2015]

13. www.adobe.com (2015). Live stream [Online] Available from: http: // www. adobe.com/devnet/adobe-media-server/articles/dynstream_ live/popup.html [Accessed: 24/02/2015]

14. www.scienceblogs.com (2009).Cognitive daily [online] Available from :http: // scienceblogs.com/cognitivedaily/2009/06/30/do-babies-like-color-if-so-whi/ [Accessed:10/06/2015]

15. https://www.askdrsears.com/topics/health-concerns/fussy-baby/science-excessive -crying-harmful[Accessed:10/06/2015]